COMPARISON OF PRESTRESSED

CONCRETE GIRDERS,

WITH DEBONDED STRANDS

AND HARPED STRANDS

by

CARMEN DÍAZ-CANEJA NIETO

Presented to the Faculty of the Graduate School of

The University of Texas at Arlington in Partial Fulfillment

of the Requirements

for the Degree of

MASTER OF CIVIL ENGINEERING

THE UNIVERSITY OF TEXAS AT ARLINGTON

May 2014

Acknowledgements

I would like to express my appreciation to Dr. Seyedali Abolmaali for his support . My appreciation extends to Dr. Yeonho Park and Dr. Swoo-Heon Lee, for their time and effort to help and guidance me throughout the experimental part of my research. I greatly appreciate Dr. Shih-Ho Chao for helping me to have a better understanding of prestressed concrete.

A special thanks needs to be extended to my husband, Brett DeVries, Family and friends for their constant encouragement, support and love. I am truly blessed to them in my life.

Additionally, I would like to thank Trinity Infrastructure LLC, Atesvi and Texas Concrete for allowing me to conduct this research. All of their employees have be helpful and friendly, but a special thanks needs to be extended to Carlos Fernández Lillo, Clara Balboa Arias and Tri Le. Their insight and help has been crucial for me to conduct this research.

April 09, 2014

Abstract

COMPARISON OF PRESTRESSED CONCRETE GIRDERS WITH DEBONDED STRANDS AND HARPED STRANDS

Carmen Díaz-Caneja Nieto

The University of Texas at Arlington, 2014

Supervising Professor: Seyedali Abolmaali

TxDOT standards follow a design that uses depressed strands for the prestressed concrete I-Girders. A new design criteria using debonded strands for prestressed concrete girders that is widely used in Europe is being introduced in Texas. This new design has been proven to be effective and faster to construct since the strands don't need to be harped.

The Lyndon B. Johnson (LBJ) Express construction project is located on I-35 and I-635 in North Dallas Texas and required placement of approximately 7,000 girders to complete this extensive project. A typical girder utilized in this project is the Tx54 with a span length of 110 feet; therefore this particular girder design was studied in this research. The testing of the girders were conducted at the precast plants of two different manufacturers: one manufacture constructed prestressed concrete girders with debonded strands and the other only prestressed concrete girders using depressed strands. For the testing, strain gauges were placed along five girders to measure the reaction of the concrete when the strands are released.

This study follows the process of construction for the two types of girders. The beams were tested at the precast plants and modeled by a finite element software to allow for comparison with tested results. This comparison will allow the safest and faster girder design for future construction projects.

Table of Contents

List of Illustrations

Chapter 1

Introduction

1.1 Introduction

1.1.1 Prestressed Concrete

Prestressed Concrete is the method in which the properties of the concrete is improved by introducing steel within the concrete. Concrete is a material known to have a high capacity to withstand compression forces, but concrete is not able to support tensile forces. On the contrary, steel is a material that is able to support tensile and compressive forces. Combining those two materials we get an element that is strong in compression but also is able to handle tensile forces. However, when a flexural load is introduced to a regular reinforced section, some cracks are developed.

To reduce the tensile stressing that are produced at the bottom, as shown in Figure 1.1, a compressive force (prestressing) is introduced to the reinforced concrete section, effectively transforming the concrete section into an elastic material.

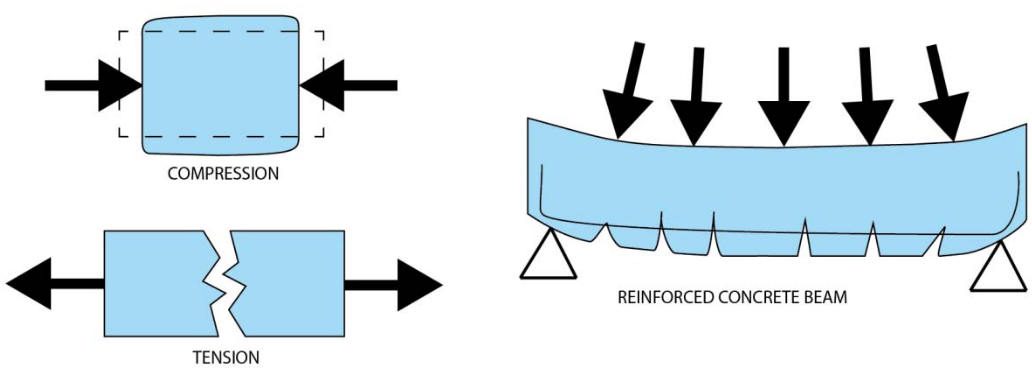

Figure 1.1: Principles of reinforced concrete.

When this method is utilized to construct the bridge girders, it is referred to as a Prestressed Concrete (PC) beams. The objective in the girders is to obtain a parabolic strand profile where the load is distributed uniformly on the concrete along the length of the strand (Figure 1.2).

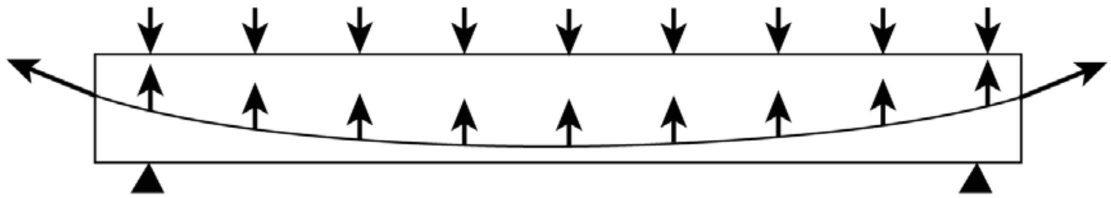

Figure 1.2: Parabolic distribution of prestressing.

The prestressing concept is not new, many examples can be found from centuries ago and in different locations throughout the world. Some of those examples are the wooden barrels (Figure 1.3) or the Totora Reed boats (Figure 1.4 and Figure 1.5) that can be found in Lake Titicaca .

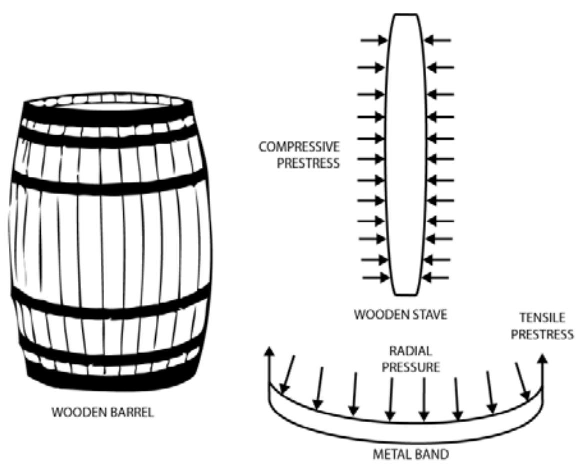

Figure 1.3: Prestressing concept for a wooden barrel.

Figure 1.4: Totora reed boats (Staples, 2006).

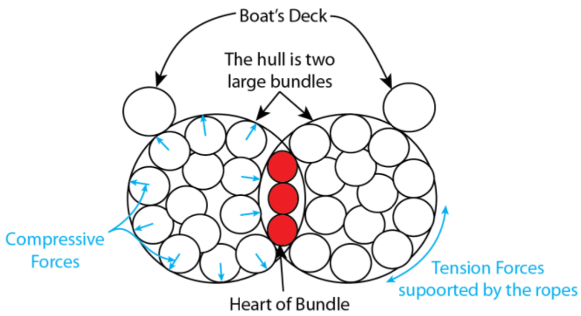

Figure 1.5: Prestressing concept of totora reed boats.

Although the prestressing concept has been around for a while, the use of PC in the United States is a relatively new concept that was introduced by Eugene Freyssinet (1879-1962). He built the first concrete bridge in the US in Pensylvania, with a centre span of 155 ft in 1949 (Naaman, 2012).

1.1.2 ABAQUS

ABAQUS is a general-purpose finite element program that was used to model the 3D model of the girders and evaluate the response.

The finite element method (FEM) is commonly used to model the behavior of PC girders and main objective for utilizing (FEM) in this study is to obtain a model that reflects the girder behavior after release.

The main advantage of creating this model is that it can be used to predict the behavior of the girder at release, which is one of the most critical steps when casting a girder.

1.2 Project Background

The Lyndon B. Johnson (LBJ) Express construction project is located on I-35 and I-635 in North Dallas Texas (Figure 1.6). When completed, this project will consist of eight lanes for general purpose traffic, two to four managed lanes, and two to three frontage road lanes. Project construction began early in 2011 and completion will occur in the summer of 2015, resulting in dramatically expanded capacity. To complete this project, approximately 7,000 girders will be placed to complete this extensive project.

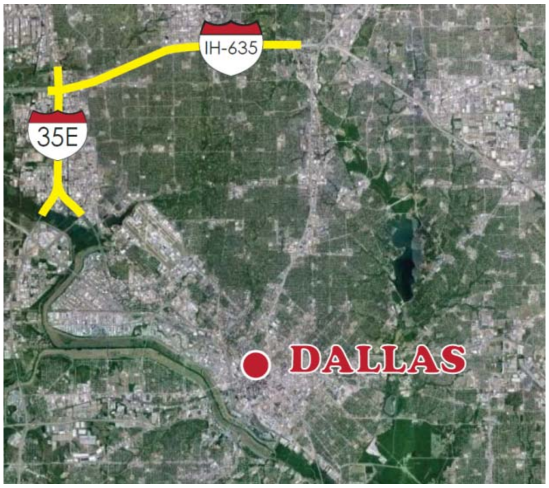

Figure 1.6: Project location (Google, Inc.).

A typical girder for this project was studied is the Tx54 with a span length of 110 feet. The testing of the girders was conducted at the precast plants of two different manufacturers: one manufacture only constructs PC girders with debonded strands and the other only constructs PC girders using depressed strands. For the testing, strain gauges were placed along four girders, two from each manufacter, to measure the reaction of the concrete when the stress from the prestressed strands were released. The strain gauges location were varied along the study, first it was focused to the girder end since is where potential cracks has seen to occur and then the strain gages were placed along the girder to measure the stress that the concrete has along the girder.

1.3 Research Objectives

The main objective of this research is to compare and analyze two typical techniques for prestressing concrete girders. The analysis is focused on the stresses that the steel transmit to the concrete when the prestressed strands are released and also the two different precast construction. The experimental data was used to verify a finite element model that can be used in the future to predict the girder behavior at release.

The following steps were conducted to achieve this objective:

1. Visit to two precast plants to observe the construction process. Both prestressing methods used to construct the girders were observed and described in this study.
2. Girder testing at the precast plants to obtain experimental data to verify the calculations and the finite element model.
3. Girder calculations were conducted to obtain the parameters needed for the finite element model.
4. Abaqus was used to create a finite element model of the behavior of the girder at release. It was focused on the transfer region of the girder.

1.4 Organization and Summary

The organization of this thesis progresses in such a way that it will allow the reader to understand basic concepts before results and conclusions are provided. In general, the layout follows the previously listed steps 1 through 4. The following provides a brief summary of each chapter within this thesis:

Chapter 2 provides information found in literature on the end girder behavior for both methods of prestressing. The two different methods of girder construction are described.

Chapter 3 describes the testing procedure that was followed to compare the behavior of both girders.

Chapter 4 provides the calculations necessary following AASHTO 2012 to model rhe girder with the finite element program Abaqus.

Chapter 5 describes the basic background information about the information used for the finite element program Abaqus to model the girder.

Chapter 6 is the chapter where general conclusions from this study are provided.

Chapter 2

Prestressed I-Girder Construction

2.1 Girder End Behavior

Prestressed girders for bridge construction is increasing being used due to their high performance and their quality/economy ratio. Strands in the concrete girders cannot be only straight and bonded because the high tensile forces transmitted to the concrete at release, would cause the girder to fail. Two different methods utilized to reduce this tensile forces which are being compared in this study are:

1. Utilizing partial debonded strands (Figure 2.1), and
2. Using harped strands (Figure 2.2).

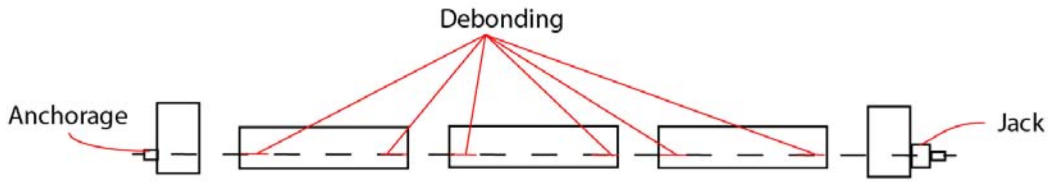

Figure 2.1: Schematic showing pretensioning of debonded strands.

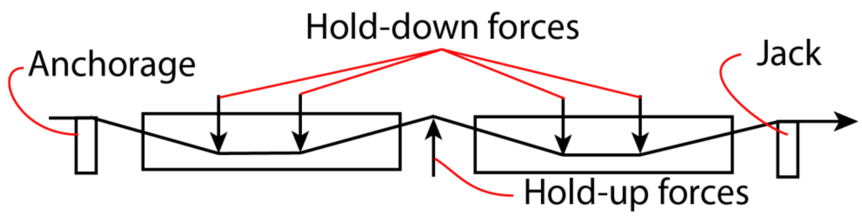

Figure 2.2: Schematic showing pretensioning with harped strands.

The use of harped strands is the common method used in Texas; however, each of these two methods has been utilized in the LBJ Express Project and each construction technique is independent. However, several cracking has been seen to develop after the release of the prestressed strands.

As a result of these developed cracking in the harped strand girders, several investigations have been conducted to identify the stresses induced by the strand releasing process. Generally, it was found that these cracks are originated by the effect of the prestress transfer that is produced when the strands are released.

Kannel, French, and Stolarski (1998) conducted a study on end cracking behavior on 45, 54, and 72 inch I-beams with draped strands. It was observed that the horizontal cracks formed at the web-flange interface were produced by stress concentrations and the strand release pattern did not affect those cracks (Kannel et al. 1998). To reduce end cracking, debonding additional prestressed strands would reduce the tensile forces (Kannel et al. 1998).

Kahl and Burgeno (2011) conducted an investigation on the effects produced by the debonded strands on the prestressed concrete beams. Since the bond strength of these debonded strands are considered zero compared to strands that are fully bonded to concrete, the stress levels at the end of the beam are less than harped strands (Kahl & Burgueno, 2011). However, cracks can occur along the entire debonded length when using flexible sheating, due to the radial expansion that is produced for the reduction of the bond strength (Kahl & Burgueno, 2011). It was stated that this damage can be only local and solely affected by confinement or reinforcement (Kahl & Burgueno, 2011).

2.2 Construction Procedure

In September 2010, Texas Department of Transportation released a new set of girder standards, for Tx40 and Tx54. The girder that it is studied is Tx54 which replaced Standard Beam type IV. The reasons for these new girder sections are:

- Improved stability,
- Wider length between girders,
- Improved durability

For the LBJ project, approximately 7,000 girders have been casted. The Tx54 type girders have been utilized extensively for the LBJ project, representing approximately 66 percent of the total girder types that has been constructed and implemented. Approximately 34 percent of these Tx54 type girders use constructed using the harped strand methods, with the remained constructed utilizing the debonded strand method of construction. The typical length for Tx54 in the project was 110 ft; therefore, conducting testing on this length of Tx54 beam is warranted. Construction sequencing for the Tx54 girders which were utilized in this research is provided subsequently.

2.2.1.1 Girder with Harped Strands Construction Sequence

The following outlines the construction sequence conducted during the construction of the Tx54 girders using harped strands:

1. Placement the bottom strands in the casting bed. These bottom strands are shown in Figure 2.3, and were either manually or mechanically placed within the casting bed.

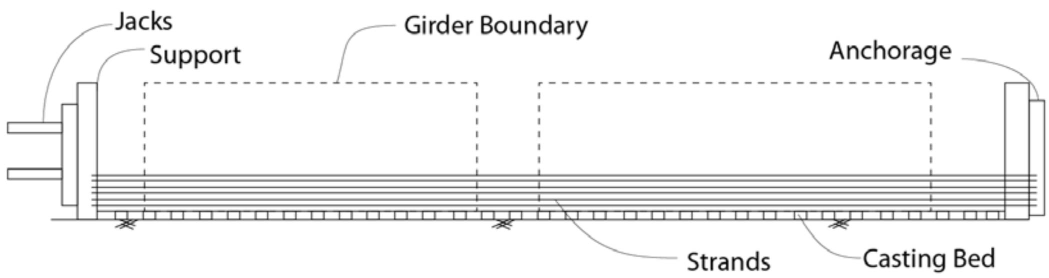

Figure 2.3: Placement of bottom strands in the casting bed

2. Placement of the harped strands. These harped strands were placed above the bottom strands within the casting bed, as shown in Figure 2.4. Similarly to the bottom strands, these harped strands were either mechanically or manually placed. The horizontal configuration of these strands was temporary, and the strands were manipulated in the subsequent construction step.

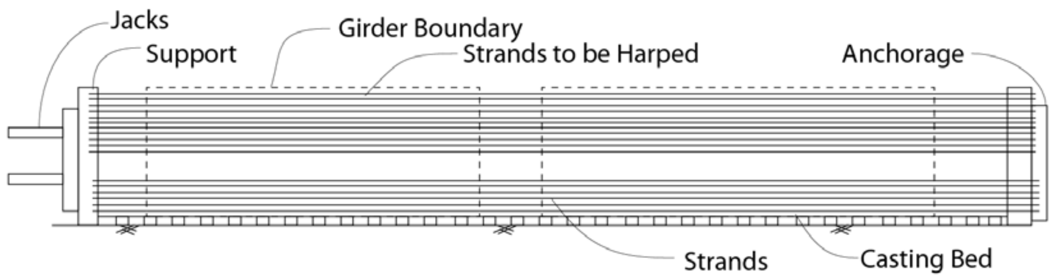

Figure 2.4: Placement of harped strands in the casting bed

3. Placement of hold-down and hold-up anchors. An uplift force of 29 kips is produced at the hold down point. The magnitude of this force has to be taken into account to ensure that the hold-down device will be able to resist this load. Typical locations of the hold-down and hold-up anchors is provided in Figure 2.6, where the hold-down anchors are normally placed within the girder limits and the hold-up anchors are positioned outside. Placement of these anchors is critical, as incorrect placement of these anchors could cause an accident.

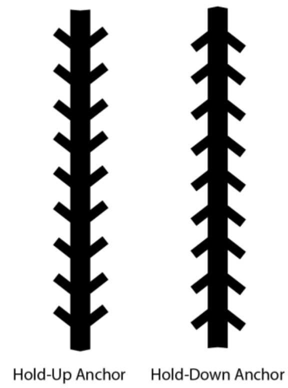

Figure 2.5: Schematic of the hold-up and hold-down anchors.

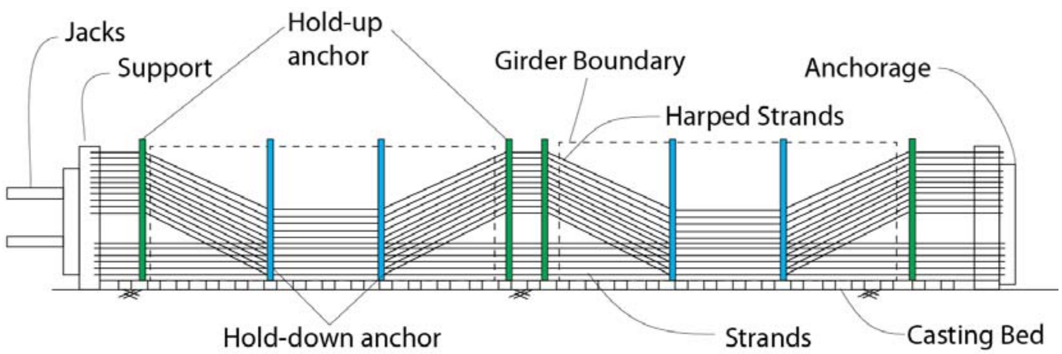

Figure 2.6: Hold-up and hold-down anchors placement within the casing bed

(construction of two girders in one casting bed).

4. Placement of Reinforced Steel. The typical reinforcement placed is shown in Figure 2.7, and is usually placed manually by a crew of 6 to 8 workers.

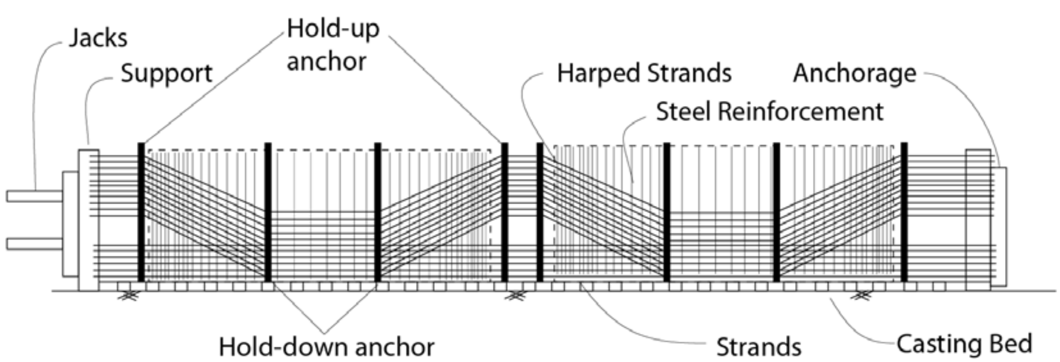

Figure 2.7: Girder with all the necessary reinforcement.

5. Stressing of the strands. An average axial force of 31 kips was placed on each strand with jacks (Figure 2.8).

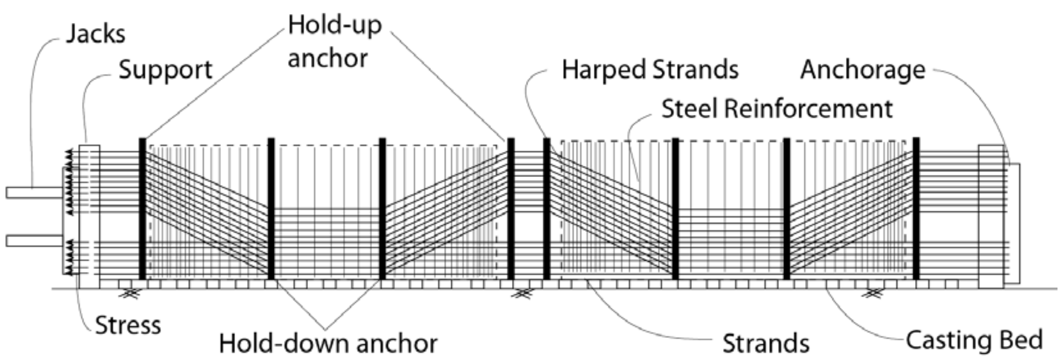

Figure 2.8:Stressing the strands

6. Placement of mold for the girder. The molds were placed with mobile cranes and allow the concrete to be poured and cured around the steel reinforcement (Figure 2.9).

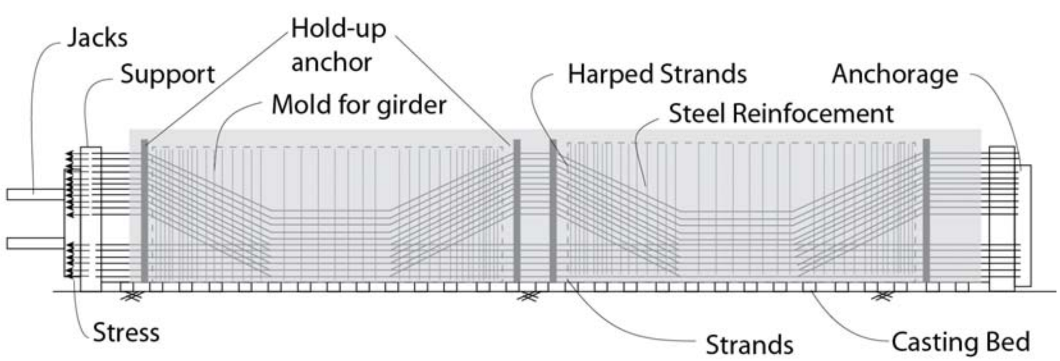

Figure 2.9: Mold placement along the girder line.

7. Concrete pouring. Qualitiy assurance was conducted during the pouring of the concrete by checking that the slump was less than 9 inches, and six cylinders were obtained to test the compression strength of the concrete.

8. Concrete curing. Wet curing was used and it usually required a cure time of at least 24 hours.

9. Concrete strength verification. The concrete cylinders obtained when the concrete is pour into the molds, were tested following ASTM Standard C39/C39M, which consisted of applying a compressive force until failure occurred. The concrete strength is obtained by dividing the load at which the concrete fails by its area.
10. Concrete block placement. If the technicians at the facility consider that the uplift force at the hold-down point locations to be too great. To prevent this, two concrete blocks, as shown in Figure 2.10 and Figure 2.11, of approximately 18,500 lbs were placed along the girder line to compensate for this uplift force.

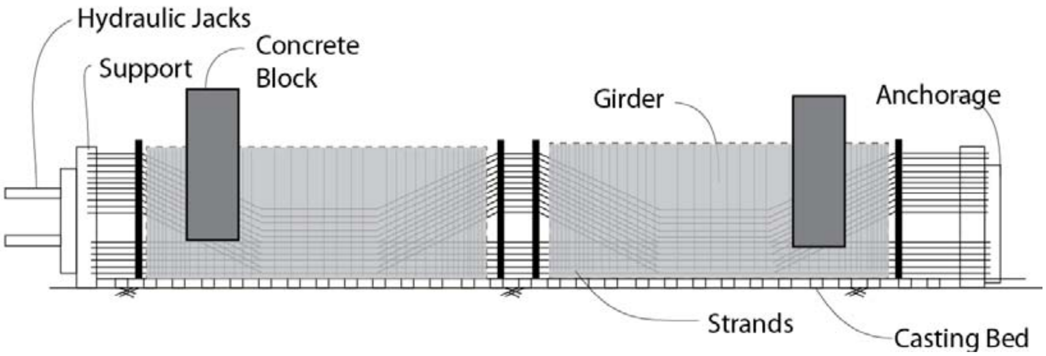

Figure 2.10: Concrete block placement before releasing the stress from the strands.

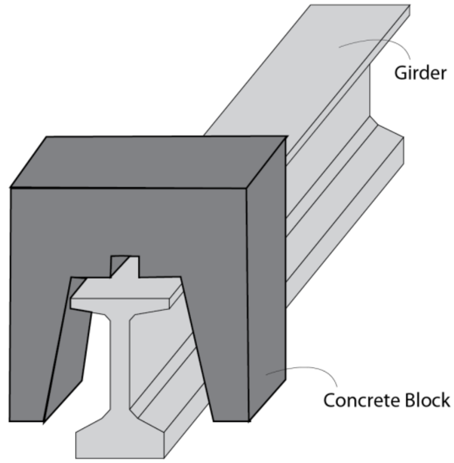

Figure 2.11: Schematic of concrete block on top of the girder.

11. Release of stress and cutting of the strands. The stress is released gradually, typically taking between 20 and 30 minutes to release all the stress placed upon the strands. Once all of the stress has been released, the strands are cut by flame cutting.

2.2.1.2 Girder with Debonded Strands Construction Sequence

The following outlines the construction sequence conducted during the construction of the Tx54 girders using debonding strands:

1. Steel reinforcement assembly. For this case, the facility had an area that was used to construct steel reinforcement cage. One or several workers can work at the same time at different locations of the girder as shown in Figure 2.12.

Figure 2.12: Steel reinforcement being assembled.

2. Steel reinforcement and strand placement in the casting bed. Once the steel cages were constructed, they were lifted and transported to the casting bed (Figure 2.13) with a crane as shown in Figure 2.14.

   The same cranes are the ones used to lift the girder after the construction of the girder was completed (Figure 2.15).

Figure 2.13: Reinforced steel after being placed in the casting bed.

Figure 2.14: Girder reinforcement being moved to the casting bed.

Figure 2.15: Girder lifting.

3. Once the cage is placed, the strands are placed in the device shown in Figure 2.16 in their respective position in the steel cage. Then a cable is hooked to the end of this device and pulling from it mechanically, the strands are placed along the girder line in an efficient and quick manner.

Figure 2.16: Device used to place the strands along the girder.

4. Stressing of strands. After all the strands are placed, the strands are stressed with a force of 44 kips per strand. (Figure 2.17)

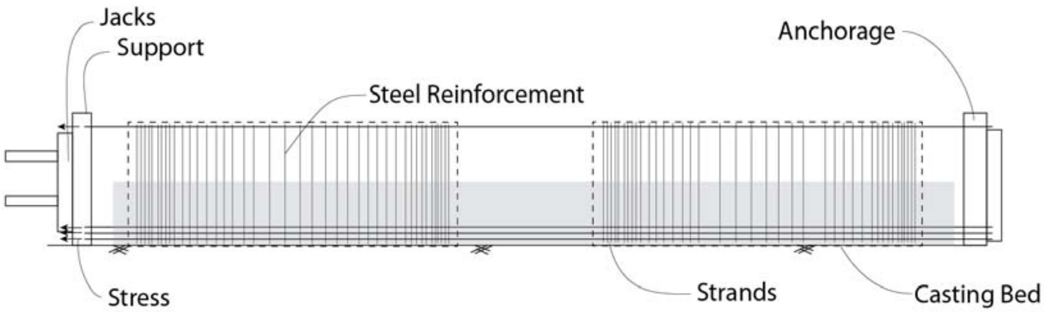

Figure 2.17: Stress of the strands

5. Placement of plastic sleeve to debond the strands. A worker is needed to place the plastic sleeve as shown in Figure 2.18. The location for the debonding is always at the end of the girder and only at the bottom strands.

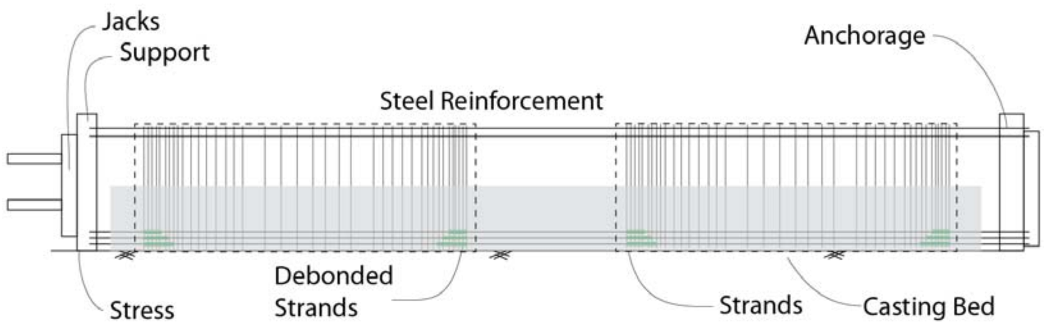

Figure 2.18: Debond strand location in the grider line.

Texas Department of Transportation requires that the ends of this plastic sleeves has to be taped, which can be time consuming since the workers do not have easy access to the strands due to the reinforcement from the steel cage. Different types of plastic sleeves have been tried to reduce the time required for plastic sleeve placement. When this testing was started, due to the type of plastic sleeve that was used, Figure 2.19. For this type of sleeve, all the debonded length was required to be taped so that the concrete didn't penetrate between the sheath and the strand.

Figure 2.19: Strand debonded.

To reduce this time, another type of plastic sleeve is being used, as shown in Figure 2.20. Instead of only one sleeve, two cylindrical sheets were used, reducing the time for its placement. Using this type of debonding, it is not needed to tape along all the debonded length, just taping the end of the length and in the center is enough to prevent the concrete from penetrating and coming in contact with the strand. Therefore, this type of sheet reduced the effort and time when debonding the strands. Figure 2.21

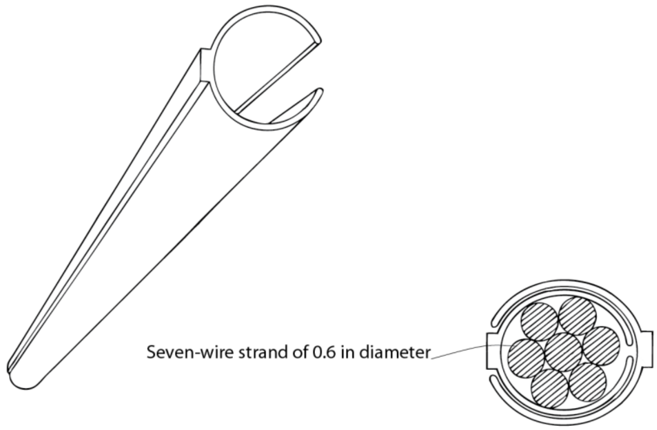

Figure 2.20: Hollow cylindrical sheet used for debonding (Coogan, 2006).

Figure 2.21: Worker placing the plastic sleeve to debond the strand.

6. Concrete pouring and vibration(Figure 2.22). Similarly to the harped strands, the slump was verified (Figure 2.23 and Figure 2.24) and six cylinders (Figure 2.25) were taken to ensure the concrete strength was adequate before release. Additionally, the temperature is checked.

Figure 2.22: Concrete pour over the girder and concrete vibration.

Figure 2.23: Worker realizing slump test.

Figure 2.24: Slump testing.

Figure 2.25: Collection of concrete cylinders.

7. Wet curing concrete. The process of curing usually took about 24 hours and used a wet matis placed along the girder line (Figure 2.26 and Figure 2.27).

Figure 2.26: End girder view with wet mat for wet curing of the concrete.

Figure 2.27: Girder line view with wet mat.

8. Concrete strength verification. The cylinders were tested following ASTM Standard C39/C39M. The test consisted of applying a compressive force until failure occurs. Dividing the load at which the concrete fails by its area, the concrete strength was obtained. Once the concrete had reached the desire concrete strength for release, the release of the stress process began.
9. Release of mold. The mold is opened with the help of a crane, as shown in Figure 2.28 and Figure 2.29.

Figure 2.28: Crane opening girder mold.

Figure 2.29: Girder mold partially opened.

10. Top strands flaming cut. The first strands were cut were those located at the top of the girder, as shown in Figure 2.30. Once the top strands were cut, the stress that is applied to the strands started gradually to be reduced with the jacks (Figure 2.31). In order to control the release, one worker had to control the stress with the gauge that is shown in Figure 2.32.

Figure 2.30: Worker flame cutting the top strands of girder.

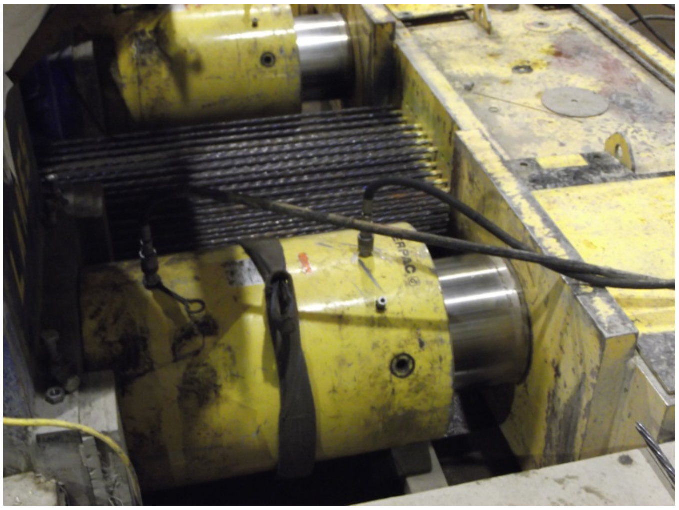

Figure 2.31: Jacks releasing the stress.

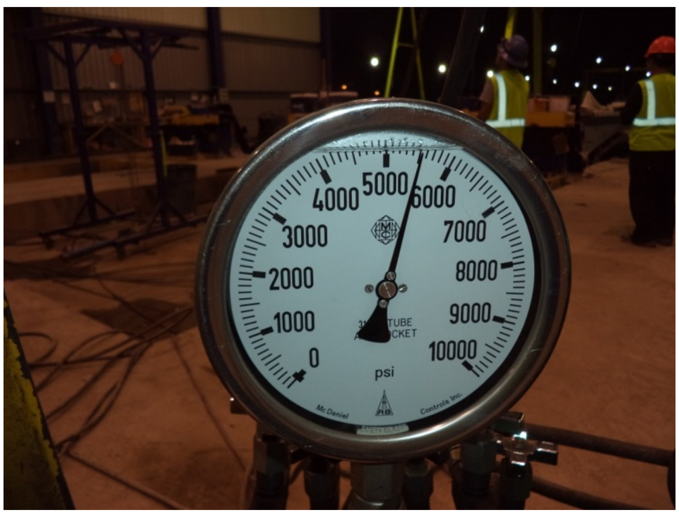

Figure 2.32: Gauge to control the release of the stress applied to the strands.

11. Release of bottom strands. Flame cutting of the bottom strands began after the release of 80 percent of the strand stress. The flame cutting was conducted by a worker at each end of the girder who were in constant contact (Figure 2.33). This ensured that the strands were flame cut in the same sequence (Figure 2.34). This cutting sequence continued until all of the bottom strands were cut and only the strands between the girders remained (Figure 2.35).

Figure 2.33: Worker flaming cut the bottom strands

Figure 2.34: View of strands after being cut.

Figure 2.35: View between girders after cutting the strands.

Chapter 3

Testing Procedure

3.1 Testing procedure description

Strain gauges were used to measure the micro-strains that occurred in the concrete when the strands within the girder were released. The subsequent steps were followed to attach the strain gauges to the girders:

1. Degrease/cleaned the area where the strain gauge were to beplaced, using aCSM-2 degreaser.
2. The surface was wetted with M-Prep Conditioner A.
3. The surface was roughened using a silicon-carbide paper.
4. A mark was placed in the location for the strain gauge for proper placement of strain gauge.
5. A reasonable amount of M-Prep Neutralizer 5A was applied and scrubbed.
6. The strain gauge was carefully removed from its envelope
7. The strain gauge was placed on the concrete at the previously marked in the location.
8. The gauge peel was removed.
9. A protective coat was applied as shown in Figure 3.1
10. This proceed was repeated and a reasonable amount of time was waited for the coat protecction to make effect before starting the testing.
11. The strain gauge was connected to a switch box, (Figure 3.3) The switch box connects the strain gauge to the strain reader (Figure 3.4). The strain reader is connected to the computer (Figure 3.5) that using an specific software it gets the readings from the strain gauges.

Figure 3.1: Coat protection over the strain gauge.

Figure 3.2: Strain gauge attached to the girder.

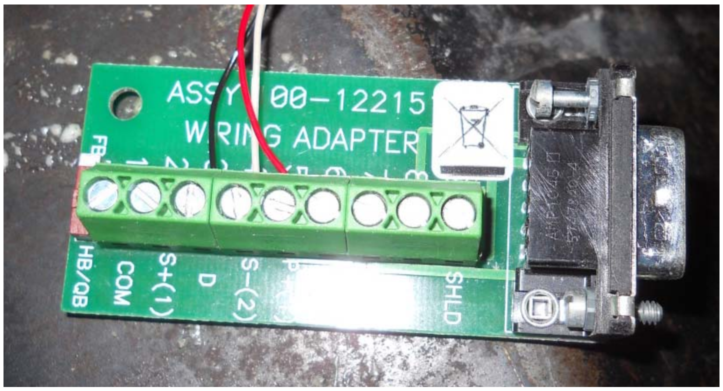

Figure 3.3: Switch box

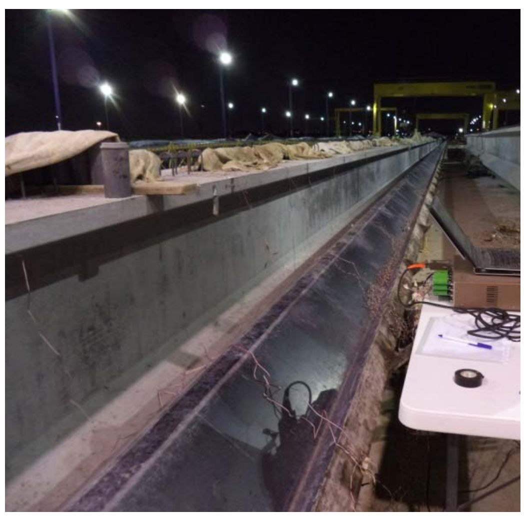

Figure 3.4: View of girder with testing equipment installed.

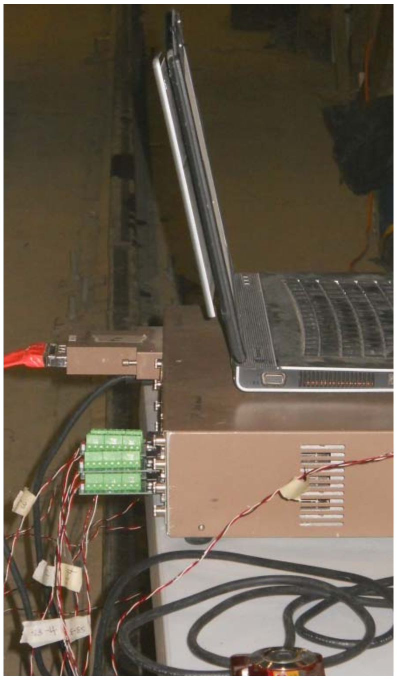

Figure 3.5: Strain reader connected to the computer.

Figure 3.6: Strain gauges on the girder.

3.2 Expected testing results

The force from the prestressing is gradually transferred from the steel to the concrete at the end of the girder. At the end of the girder the steel is considered to transfer zero stresses and progressively transfer all the prestress to the concrete. Section 4.2. explains the idealized relationship between steel stress and distance from from the end of the girder.

Since most of the strands are located at the bottom of the girder, higher compression strain is expected in that region. Tension strains can be expected at the top of the girder due to the effect of the prestress and the effect self-weight of the girder.

3.3 First Monitoring

The first monitoring was conducted on one Tx54 girder with debonded strands. Fifteen strain gauges were placed on concrete at the end of the girder, exactly at 54 inches from the (Figure 3.7). strain gauges were labeled for the section and row in which they were placed (i.e., the strain gauge placed in Section 1 and row 3 would be labeled [1-3]).

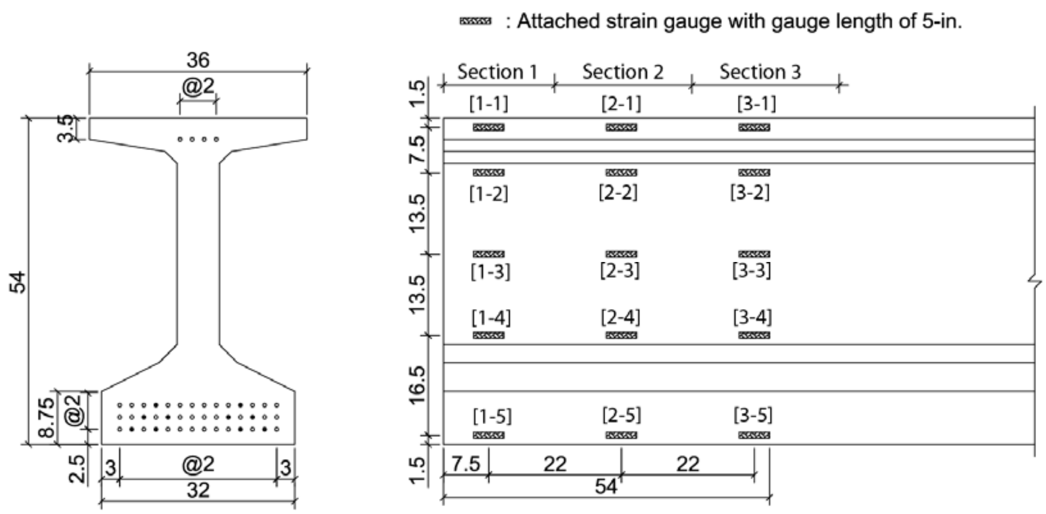

Figure 3.7: Strain location for the first monitoring (units in inches).

The last row of strain gauges were not installed due to the conditions present at the time of monitoring, with the mold attached at the casting bed. Placement of these strain gauges would have been time consuming and resulted in an unacceptable girder construction delay; therefore, these strain gauges were not placed.

Results from strain gauges located in Section 1 is provided in Figure 3.9. Strain [1-4] shows an abrupt increase in strain (tension) immediately before the flame cutting of the strands on top of the girder finished. This can be explained by a concrete failure in that area, potentially leading to the development of a. It should be noted that microcracks (Figure 3.8) have been observed in previously constructed girders with the same design. Alternatively, this result can also be explained by a malfunction in the strain gauge. Strain gauges [1-2] and [1-3] experienced the expected compression, varying lineally with no abrupt changes. Strain gauge [1-1] experienced relatively small amounts of change in strain during all the release process.

Figure 3.8: Microcraks at girder end.

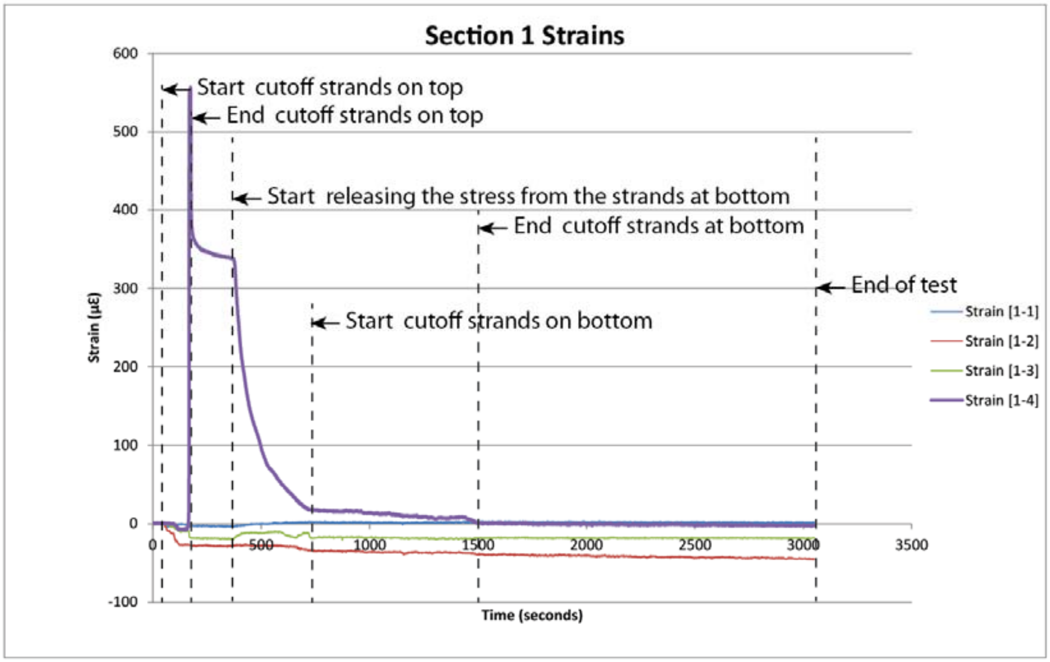

Figure 3.9: Strain gauges located at section 1.

Strain gauge results from Section 2 during the first monitoring period are provided in Figure 3.10. Similar but not as great strains as strain gauge [1-4] are shown in strain gauge [2-4] (i.e., the concrete experienced tension at the beginning of the monitoring period followed by an abrupt drop in strain to compression following the end of the flame cutting of the top strands). Monitoring results from strain gauge [2-3] are drastically different than what should theoretically occur (i.e., the strain gauge results showed that the concrete is experiencing tension when there should theoretically be compression in that region). Strain gauge [2-2] showed an abrupt change in compression, which can be interpreted that the concrete has failed, potentially leading to the appearance of microcracks. An abrupt change in strain at multiple strain gauges occurs at the end of the flame cutting of the top strands leads, leads to the conclusion that this phase of the construction sequence should be modified to prevent the development of microcracks in the girder.

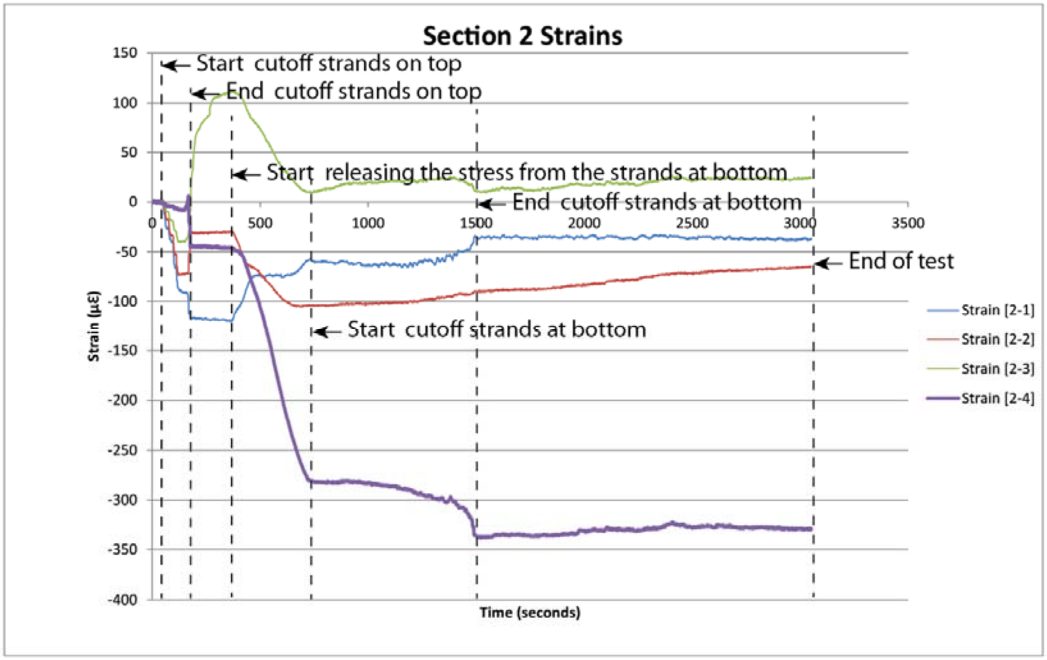

Figure 3.10: Strain gauges located at section 2.

Figure 3.11 represents the results obtained from the strain gauges located in Section 3. All the strain gauges, except [3-4] showed a linear variation (i.e., no abrupt change in the strain results) of the concrete. Strain gauge [3-4] showed more variation in the concrete; however, these changes in the strains were relatively small compared to other sections.

A general conclusion can be made that the abrupt change in strains at the end of the flame cutting of the top strands is greater the closer the strain gauges were to the end of the beam at the start of the web.

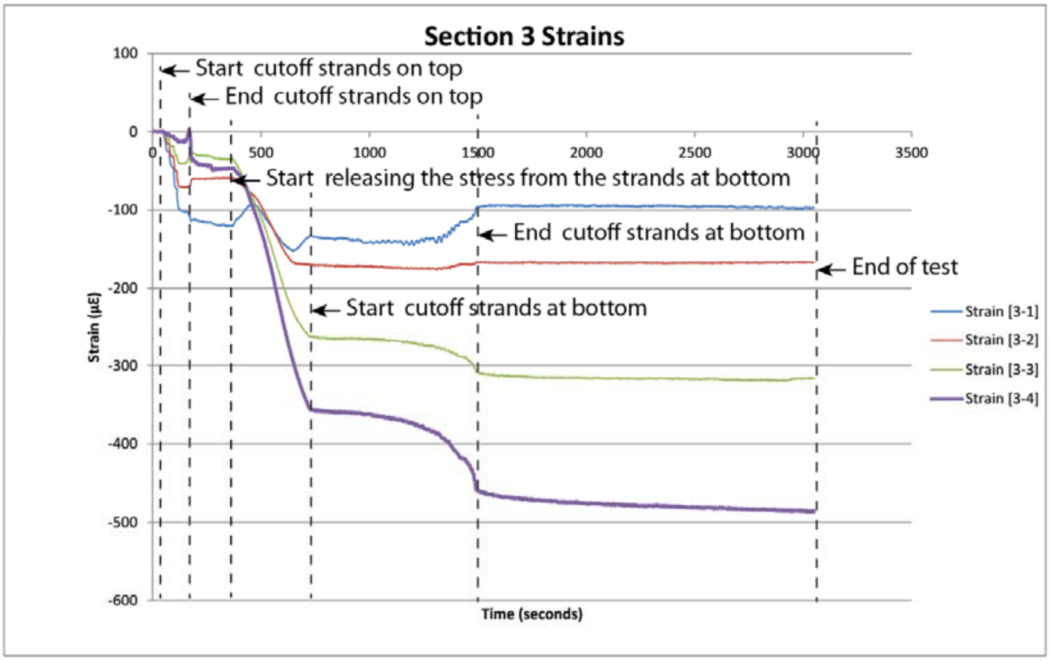

Figure 3.11: Strain gauges located at section 3.

3.4 Second Monitoring

The second testing incorporated both the harped and debonded strands for the Tx54 girder with a length of 110 feet. Seventeen strain gauges were attached in each of the two prestressed girders at the same location. It should be noted that two concrete blocks were placed along the girder line for the harped strands girder. As a result of the first monitoring results, which showed that the critical motoring locations were at the edges of the girder, greater amounts of strain gauges were placed at these locations. The resulting strain gauge locations for the second monitoring of both types of Tx54 girders is provided in Figure 3.12.

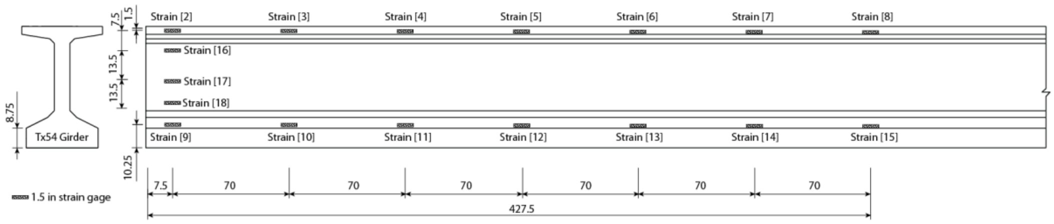

Figure 3.12: Strain gauge locations for the second monitoring.

Strain gauge results from the second monitoring of the Tx54 girders are provided in Figure 3.13 through Figure 3.29. These figures present a comparison between strain gauges at the same location of the girder for two types of prestressing method. The results cannot be directly compared because the timing for the release varied between the two girders. However, the strain gauge reading at the end of the monitoring period between the two girders can be compared.

General conclusions from the second monitoring of the debonded and harped strand Tx54 girders are as follows:

1. Some strain gauges at the end of the girder showed that the concrete was subjected to tensile forces at the release for both cases. These results are similar to those obtained from the first monitoring.
2. The strain gauges at the end of the girder for the debonded girders showed an abrupt tension strain variation (similar to the first monitoring) when the flame cutting of the top of the strands was completed.
3. Harped girder strain gauges tended to monitor a noise strain variation when the compression from the girder was supposed to be released but prevented by the concrete block.
4. The top of the girder strain gauges showed higher strains for the harped strands girders when compared to the debonded strands (Figure 3.30).

5. Strain gauges at the bottom of both types of girders did not show a significant variation in strains (Figure 3.31).
6. Strains monitored at the end of the girder showed tension and compression behavior at the same section (Figure 3.32), which was in agreement with the first monitoring.

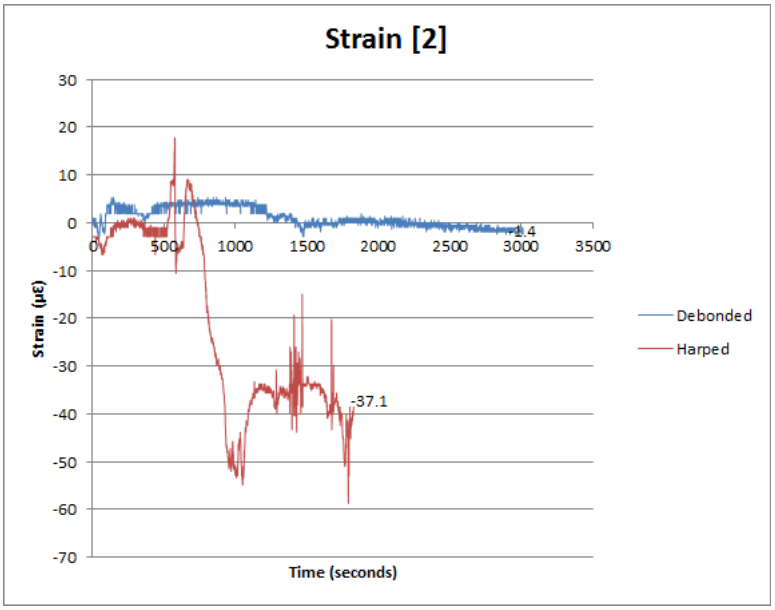

Figure 3.13: Strain gauge [2] readings for both types of girders.

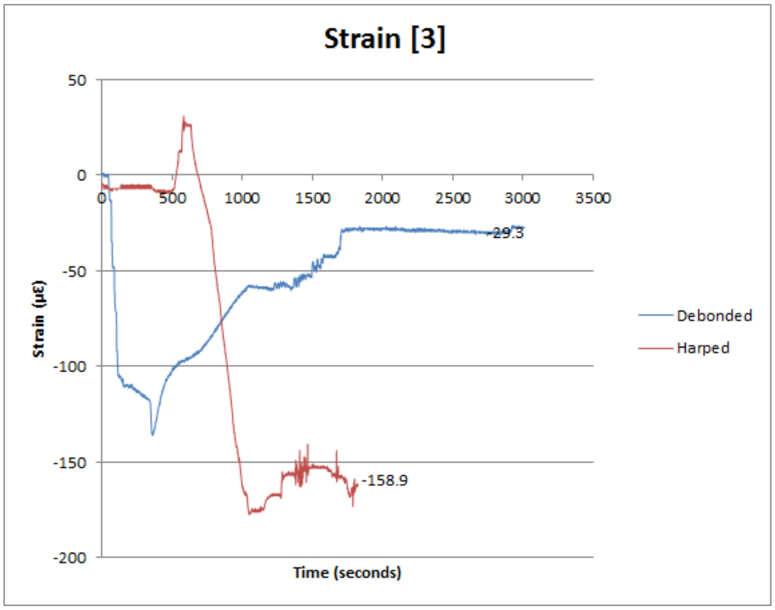

Figure 3.14: Strain gauge [3] readings for both types of girders.

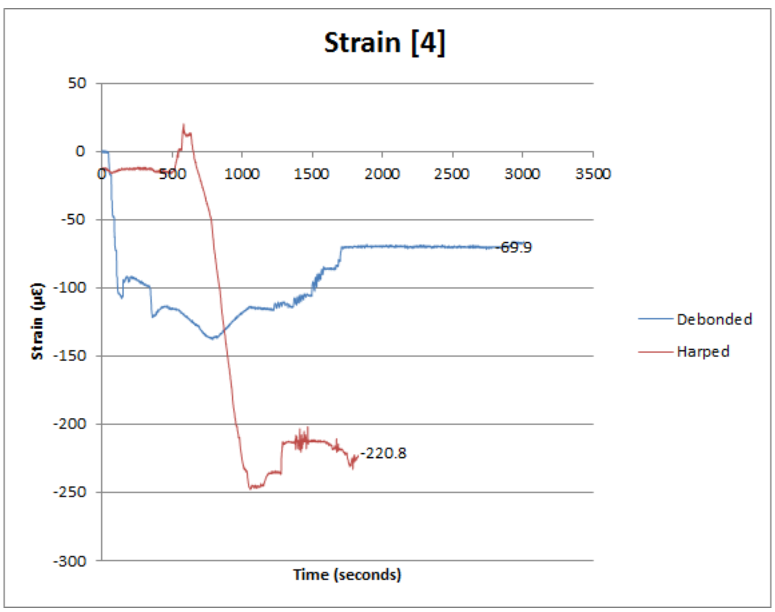

Figure 3.15: Strain gauge [4] readings for both types of girders.

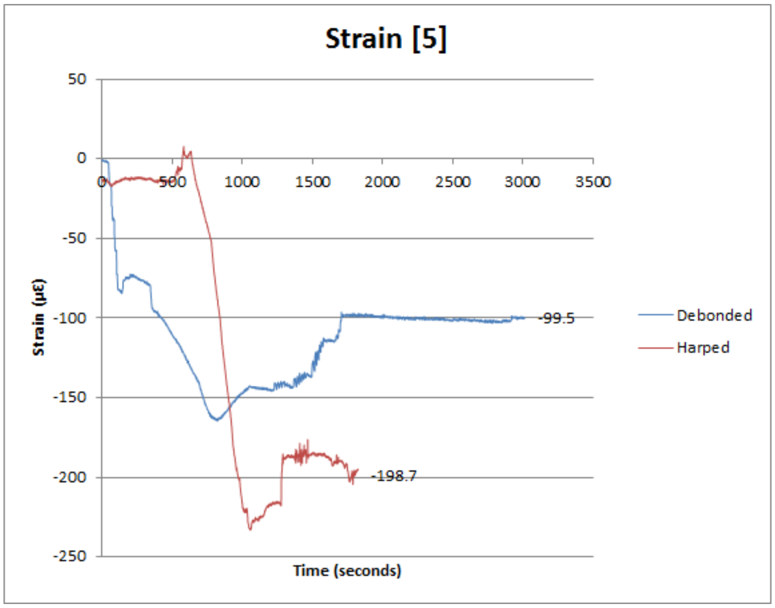

Figure 3.16: Strain gauge [5] readings for both types of girders.

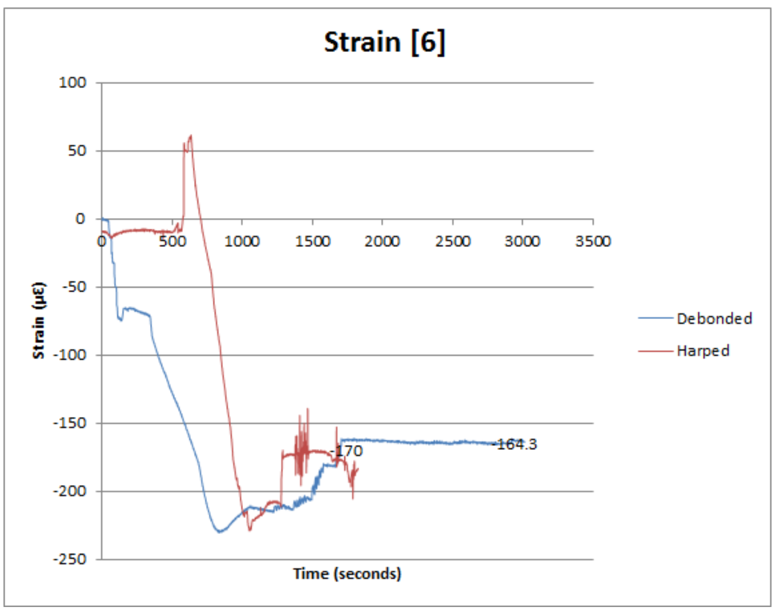

Figure 3.17: Strain gauge [6] readings for both types of girders.

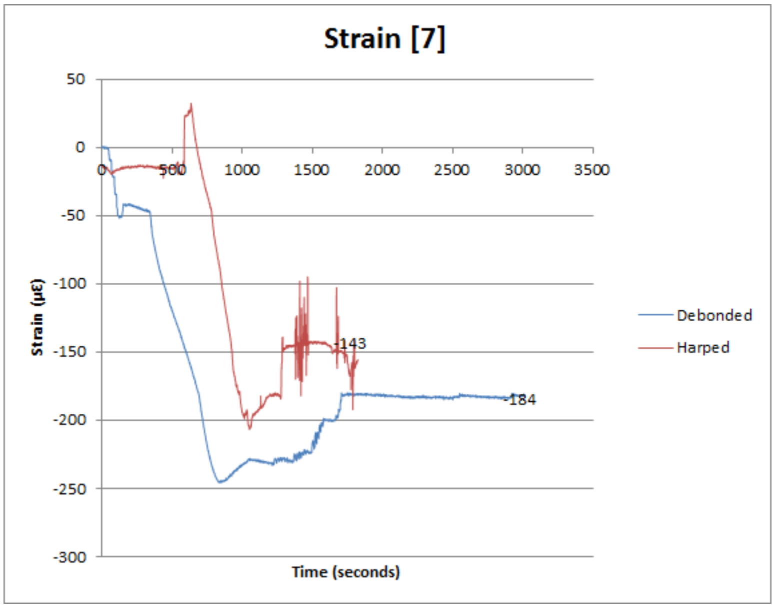

Figure 3.18: Strain gauge [7] readings for both types of girders.

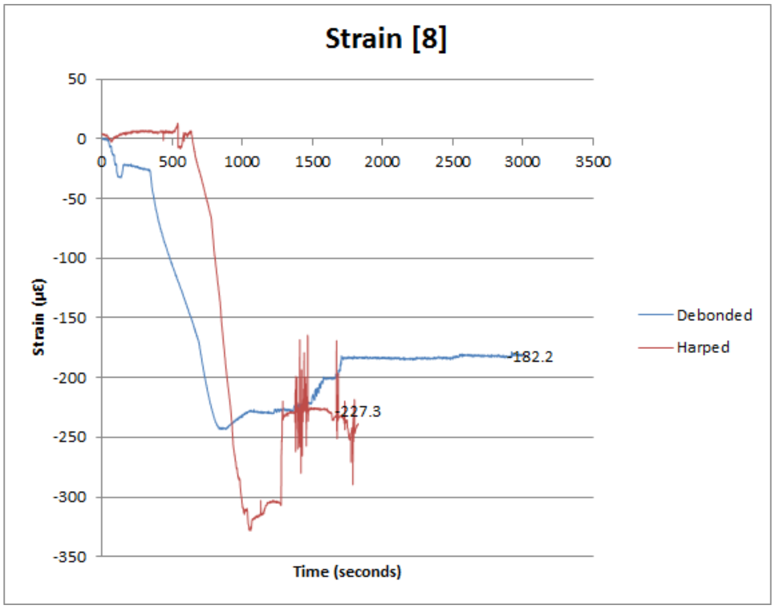

Figure 3.19: Strain gauge [8] readings for both types of girders.

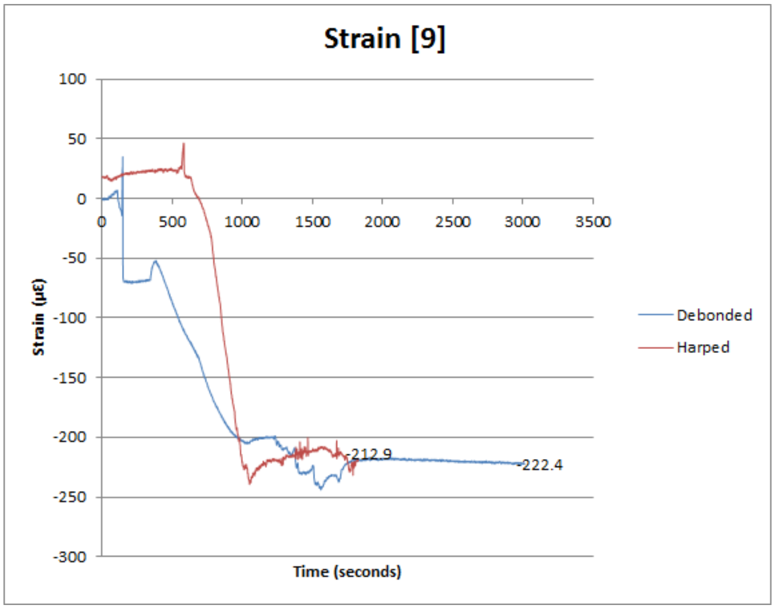

Figure 3.20: Strain gauge [9] readings for both types of girders.

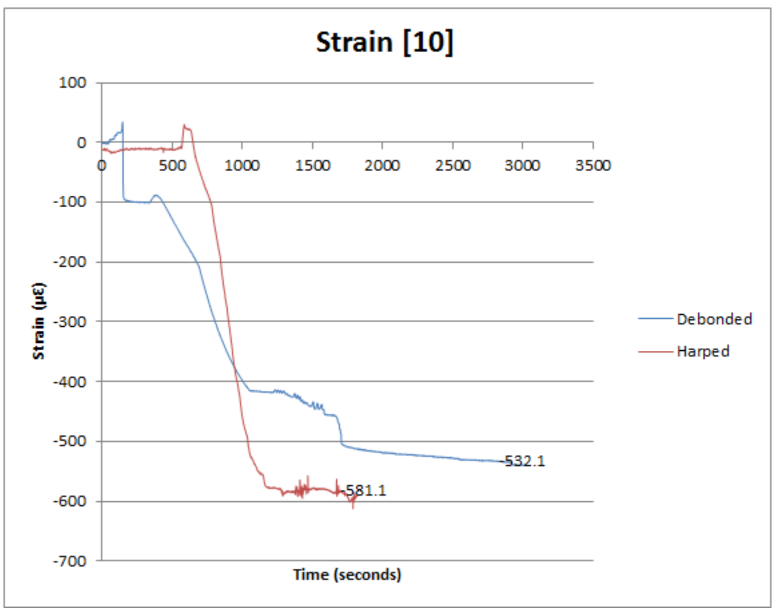

Figure 3.21: Strain gauge [10] readings for both types of girders.

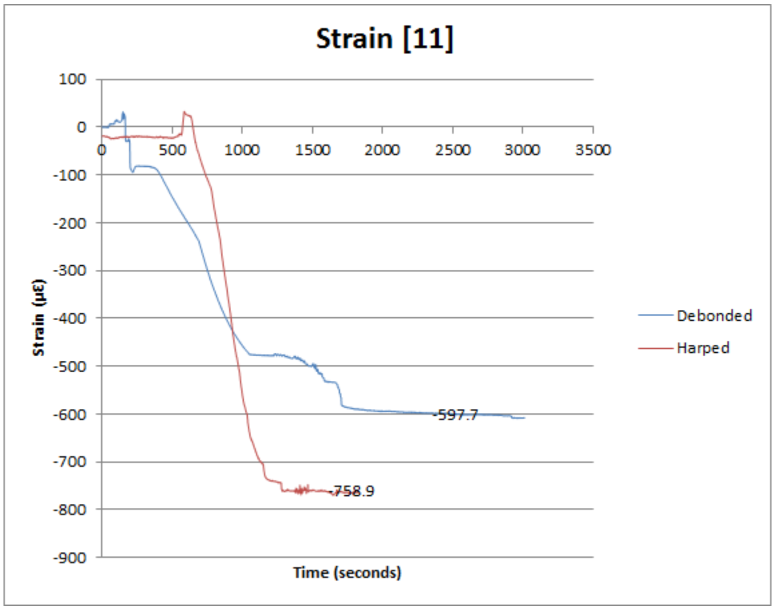

Figure 3.22: Strain gauge [11] readings for both types of girders.

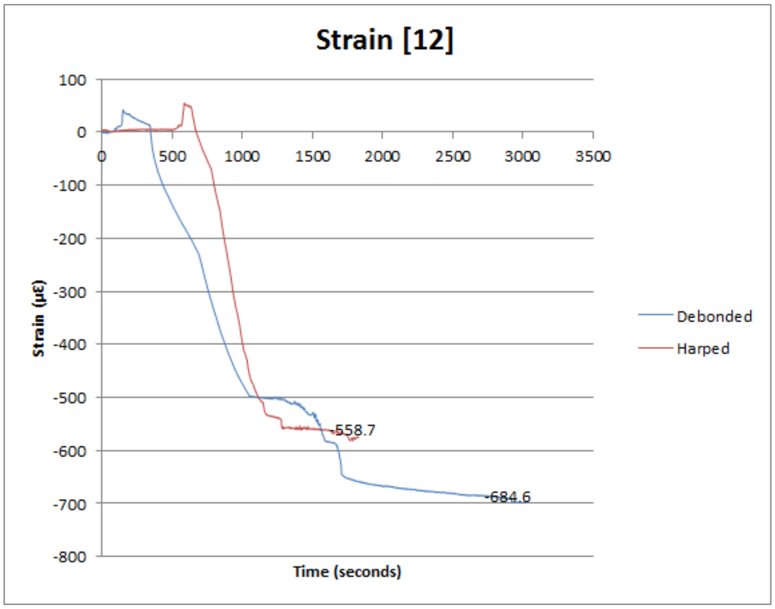

Figure 3.23: Strain gauge [12] readings for both types of girders.

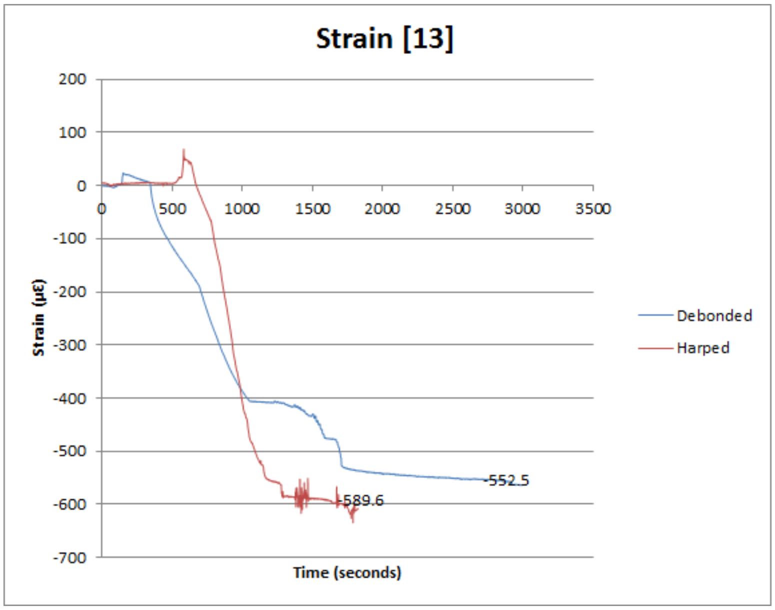

Figure 3.24: Strain gauge [13] readings for both types of girders.

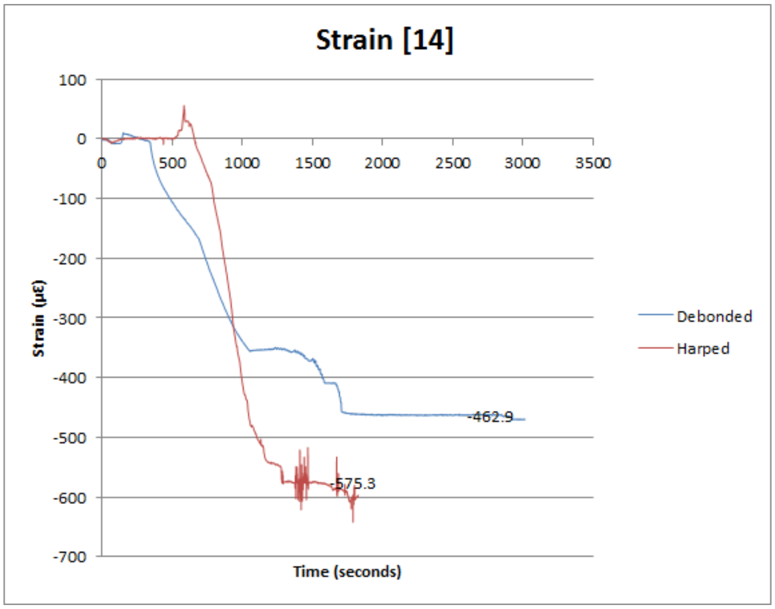

Figure 3.25: Strain gauge [14] readings for both types of girders.

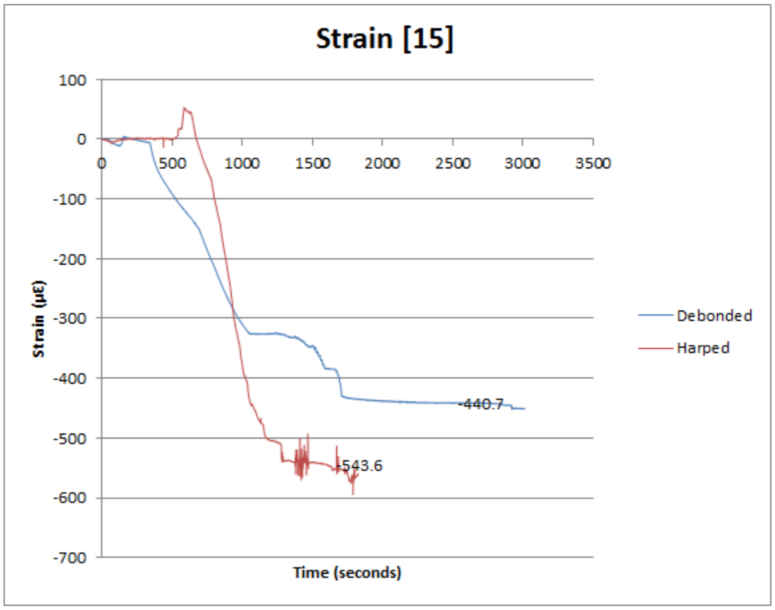

Figure 3.26: Strain gauge [15] readings for both types of girders.

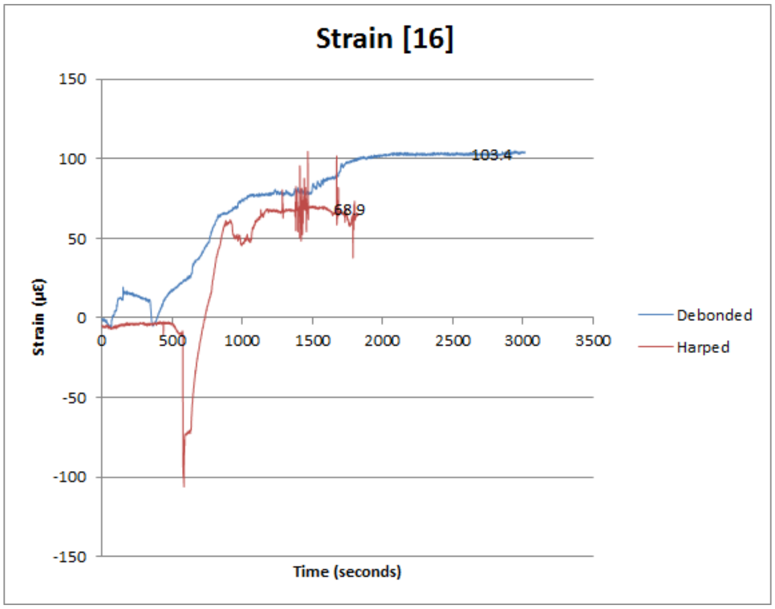

Figure 3.27: Strain gauge [16] readings for both types of girders.

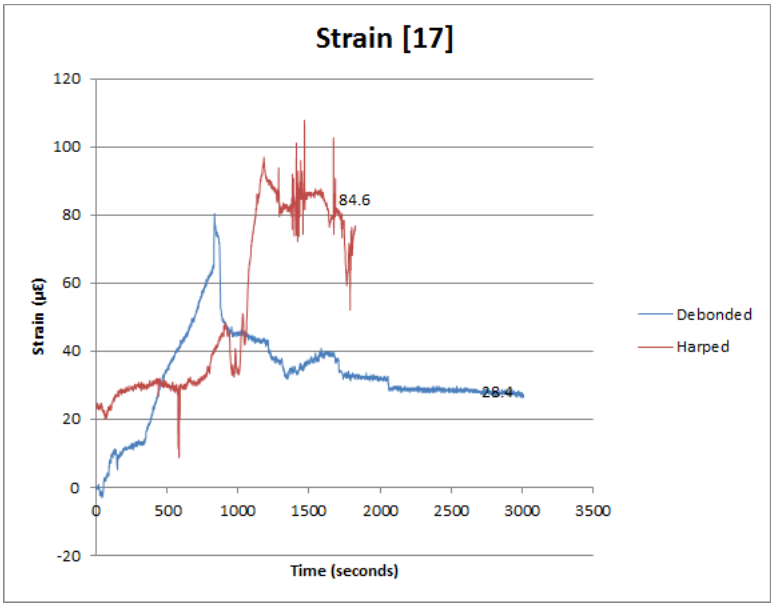

Figure 3.28: Strain gauge [17] readings for both types of girders.

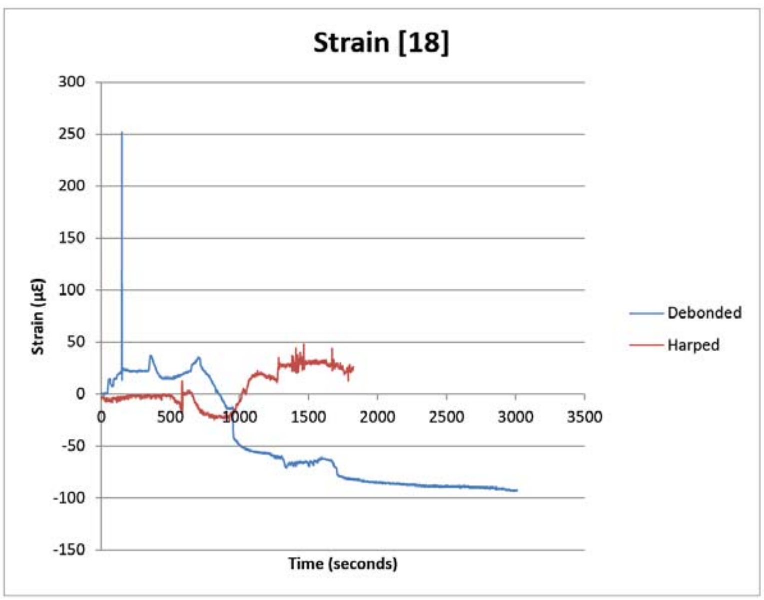

Figure 3.29: Strain gauge [18] readings for both types of girders.

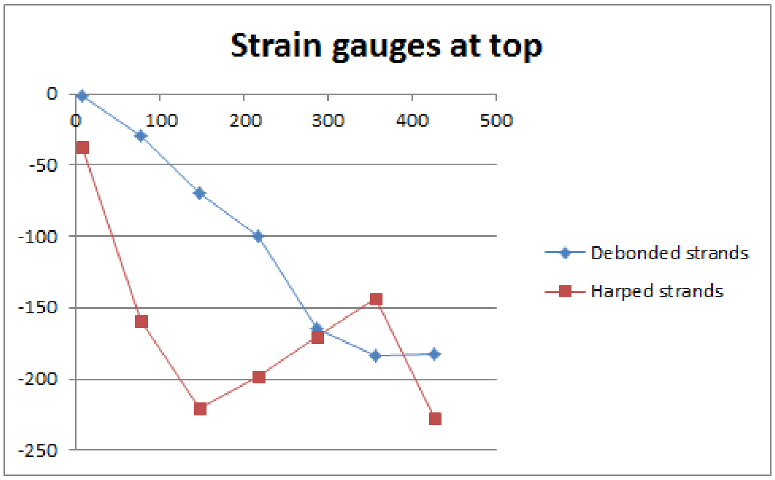

Figure 3.30: Values for strain gauges [2], [3], [4], [5], [6], [7] & [8].

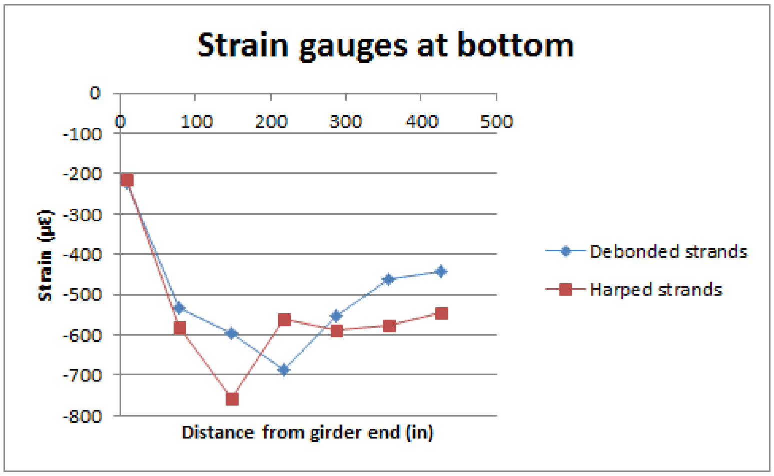

Figure 3.31: Values for strain gauges [9], [10], [11], [12], [13], [14] & [15].

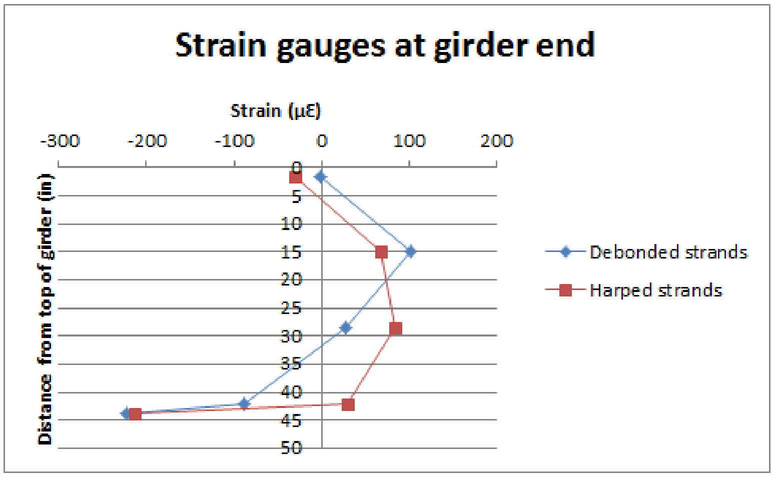

Figure 3.32 Strain gauges [2], [16], [17], [18] & [9] values.

3.5 Third Monitoring

The third testing was followed a similar testing method as the second monitoring; however, eleven strain gauges were attached only to the bottom flange of each Tx54 girder. Additionally, the concrete block was not placed on top of the harped strands girder. Locations of the strain gauges for both of the girders is shown in Figure 3.33.

Results for the third monitoring are provided in Figure 3.34 through Figure 3.44. Similarly to the second monitoring, a comparison between the harped and debonded girders cannot be directly be compared because of variations in release timing. However, the final strain gauge result between the two girders can be compared.

Conclusions and comparisons between the two other monitoring periods (first and second) are stated as follows:

1. Very similar results and conclustions are gathered from the third monitoring as the second.
2. The girder with harped strands did not present a noise variation in the strains; therefore, the conclusion made during the second monitoring

about the concrete block causing this variation can be considered accurate.

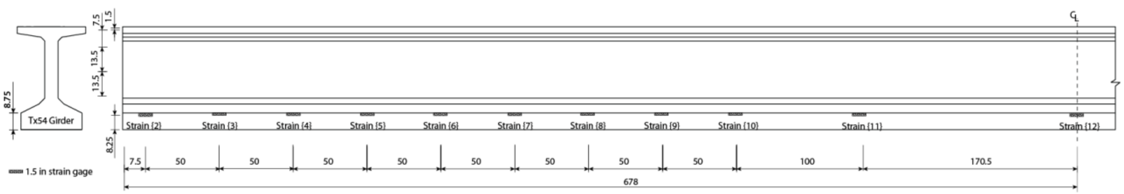

Figure 3.33: Strain location for the third monitoring.

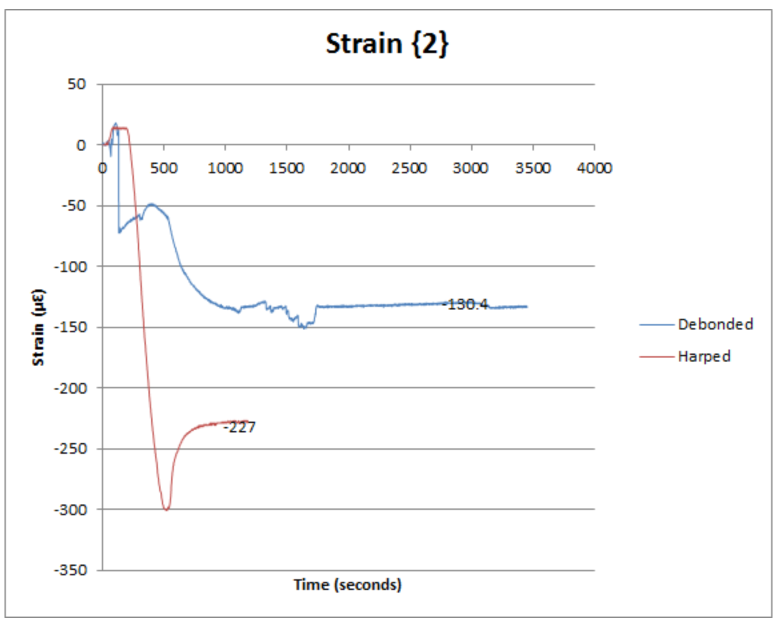

Figure 3.34: Strain gauge {2} readings for both types of girders.

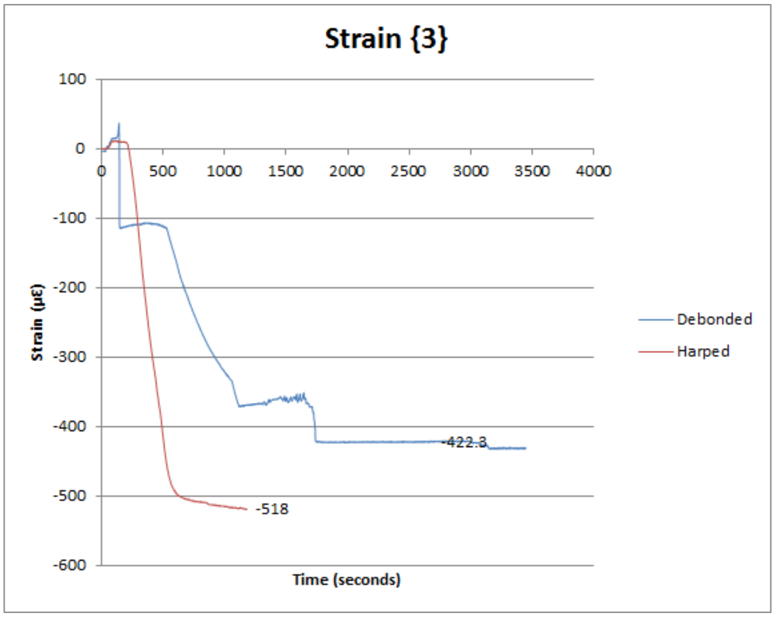

Figure 3.35: Strain gauge {3} readings for both types of girders.

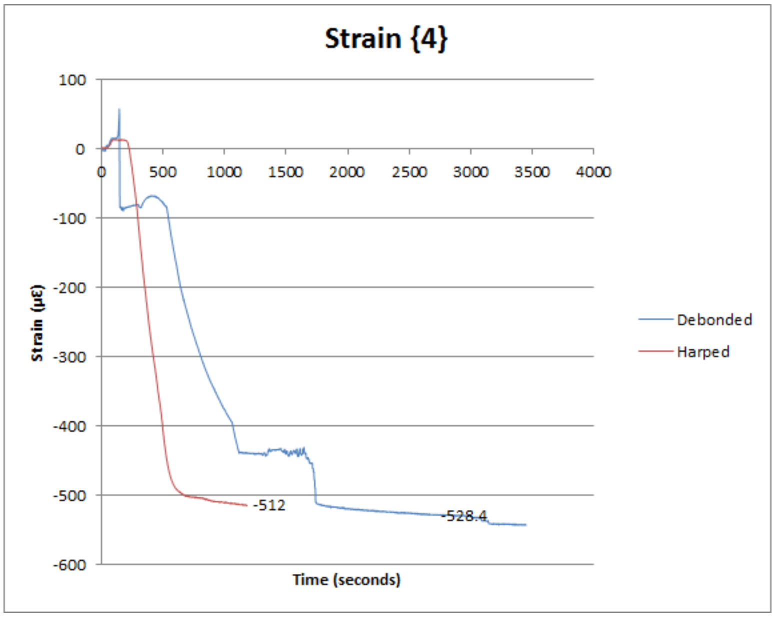

Figure 3.36: Strain gauge {4} readings for both types of girders.

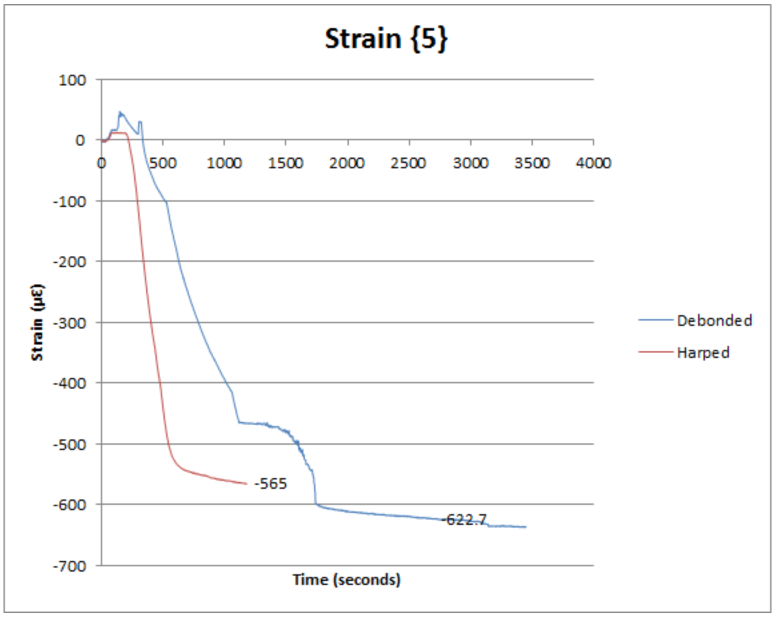

Figure 3.37: Strain gauge {5} readings for both types of girders.

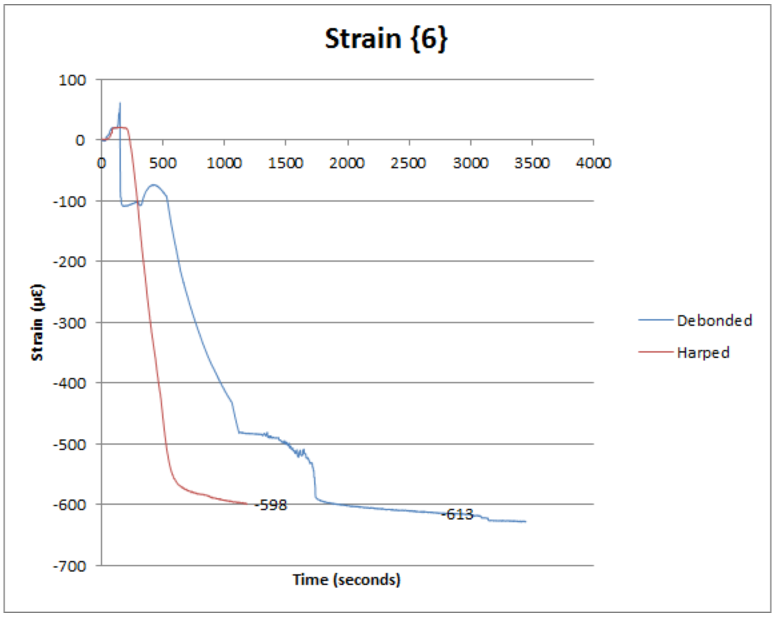

Figure 3.38: Strain gauge {6} readings for both types of girders.

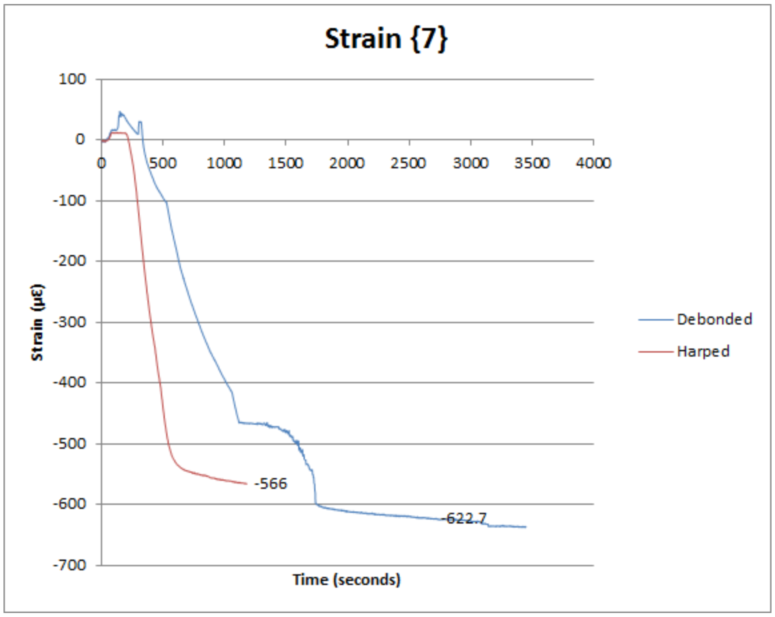

Figure 3.39: Strain gauge {7} readings for both types of girders.

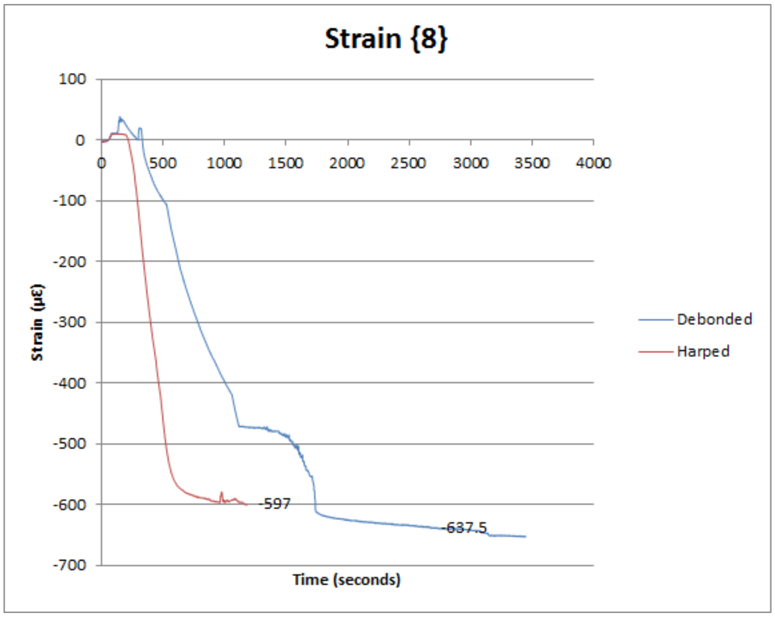

Figure 3.40: Strain gauge {8} readings for both types of girders.

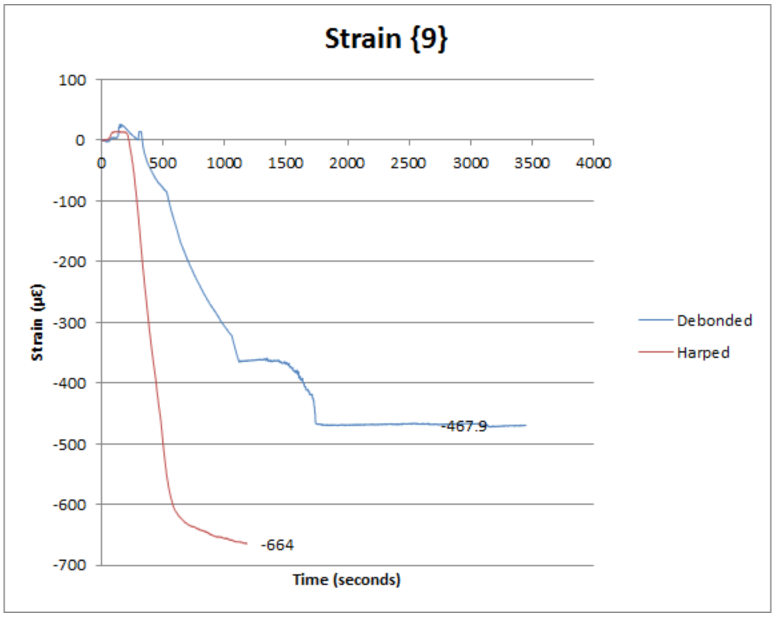

Figure 3.41: Strain gauge {9} readings for both types of girders.

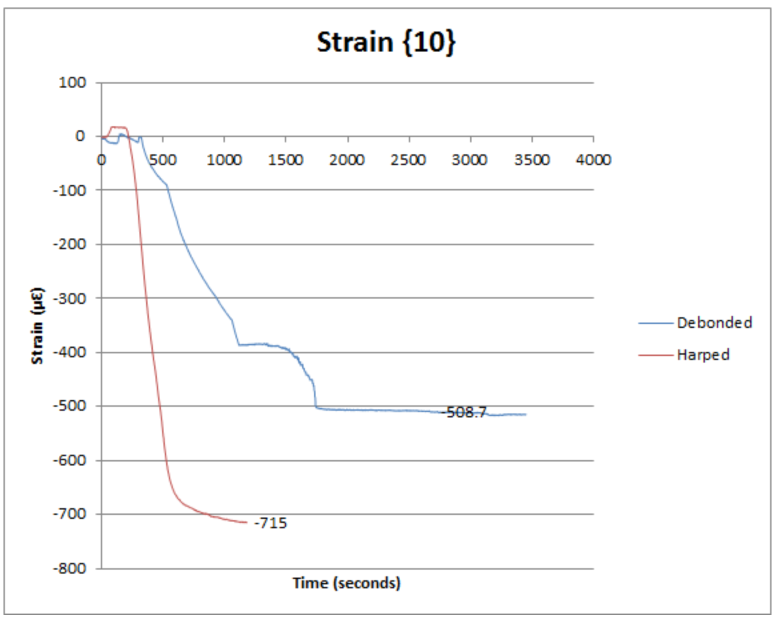

Figure 3.42: Strain gauge {10} readings for both types of girders.

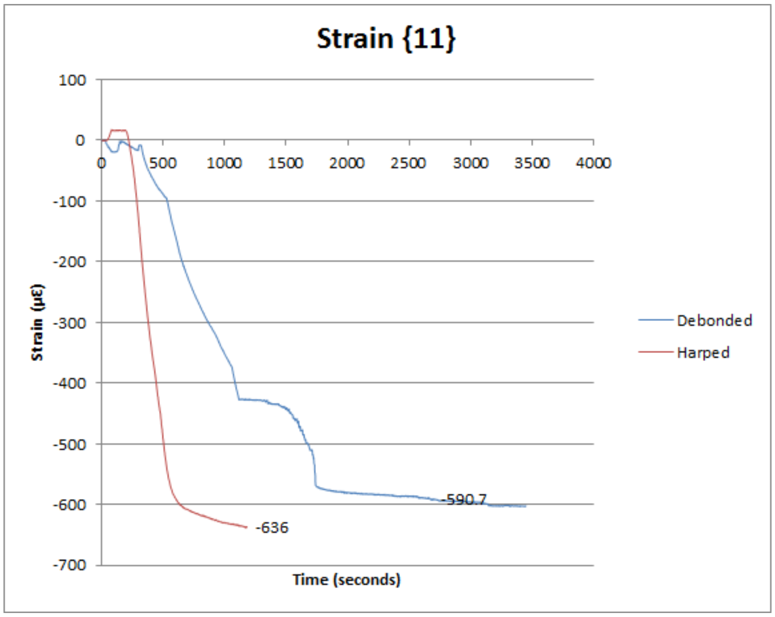

Figure 3.43: Strain gauge {11} readings for both types of girders.

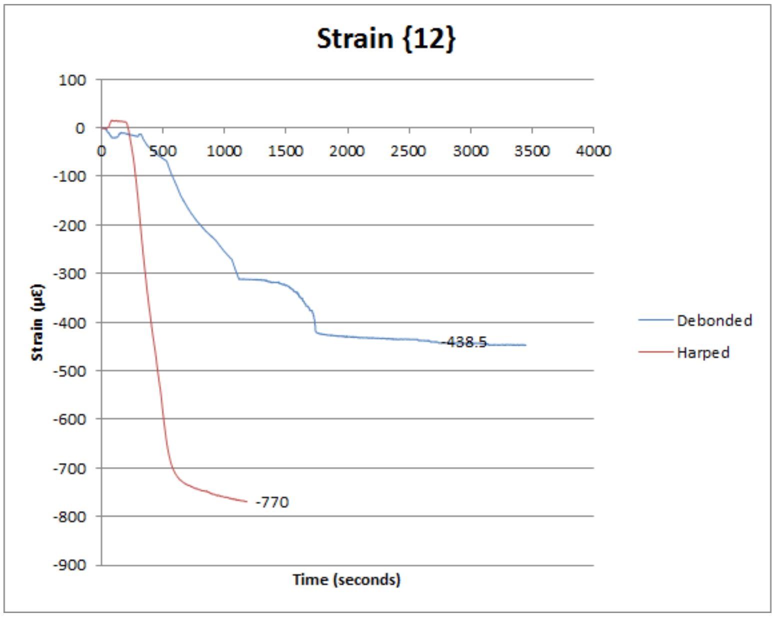

Figure 3.44: Strain gauge {12} readings for both types of girders.

Chapter 4

Girder Design

The design and revision process for the LBJ Express Project can be summarized as follows:

1. Preliminary girder design following AASHTO LRFD Bridge Design Specifications and Texas Department of Transportation Standards is conducted by consulting firms working for Trinity Infrastructure.
2. The preliminary design is reviewed and approved by Trinity Infrastructure.
3. Issued for construction drawings are produced by the preliminary girder design consulting firms.
4. These drawings are sent to manufacturing plants to produce the girders.
5. The manufacturing plant companies are allowed to improve the design, following the AASHTO LRFD Bridge Design Specifications. The production shop drawings that will be used for the casting of the girder is sent to the technical office in Trinity Infrastructure.
6. These shop drawing are reviewed, revised, and approved by Trinity Infrastructure. Once these drawings are approved, casting of the girders can be conducted.

As a result of the AASHTO LRFD Bridge Design Specifications being significantly utilized in the design of the girders for the LBJ Express Project, these specifications will also be used for this research. The subsequent calculation procedure was based on girder specifications provided by the shop drawings (APENDIX B) from the precast plants and include the following:

- Diameter of the strands (Ø),

- Total number of strands,
- Number of strands harped or debonded,
- Tensile strength of prestressing steel (f_{pu}),
- Type of tendon,
- Compressive strength of concrete (f'_c),
- Compressive strength of concrete at release (f'_{ci}),
- Eccentricity at center line of girder (e_{cl}), and
- Eccentricity at end of girder (e_{end}).

4.1 Prestress losses

For the purpose of this study, it is important to estimate the prestress losses that occur after transfer of stress from the steel to the concrete. f_{pe} will be considered as the stress remaining after all losses have occurred at release. For pretensioned member, the total losses are computed as (AASHTO, 2012):

$$\Delta f_{pT} = \Delta f_{pES} + \Delta f_{pLT} \tag{1}$$

Where; Δf_{pT} is the total loss (ksi), Δf_{pES} is the sum of all losses or gains due to elastic shortening or extension at the time of application of prestress and/or external load (ksi) and Δf_{pLT} is the sum of the losses due to long-term shrinkage and creep of concrete and the relaxation of steel (ksi).

4.1.1 Elastic Shortening

This elastic shortening can be calculated as follows (AASHTO, 2012):

$$\Delta f_{pES} = \frac{E_P}{E_{ct}} f_{cgp} \tag{2}$$

According to section C5.9.5.2.3a of AASHTO (2012), the loss due to elastic shortening in pretensioned member may be determined by the following alternative equation (AASHTO, 2012):

$$\Delta f_{pES} = \frac{A_{ps} \cdot f_{pbt} \cdot (I_g + e_m{}^2 \cdot A_g) - e_m \cdot M_g \cdot A_g}{A_{ps} \cdot (I_g + e_m{}^2 \cdot A_g) + \frac{A_g \cdot I_g \cdot E_{ci}}{E_p}} \quad (3)$$

Where; A_g is the gross area of section and E_{ci} is the modulus of elasticity of concrete at transfer

E_{ci} is the modulus of elasticity of concrete at transfer as (AASHTO, 2012):

$$E_{ci} = 33{,}000 \cdot K_1 \cdot w_c{}^{1.5} \sqrt{f'_{ci}} \quad (4)$$

Where; K_1 is the correction factor for source of aggregate to be taken as 1.0 unless determined by physical test, and as approved by the authority of jurisdiction (AASHTO, 2012) ,w_c is the unit weight of concrete, E_p is the modulus of elasticity of prestressing tendons, e_m is the average prestressing steel eccentricity at midspan. f_{pbt} is the stress in prestressing steel immediately prior to transfer. According to Table 5.9.3-1 (AASHTO, 2012), for low relaxation strands, the stress limit is $f_{pbt} = 0.75 \cdot f_{pu}$, where f_{pu} is the tensile strength of prestressing steel. I_g is the moment of inertia of the gross concrete section and M_g is the midspan moment due to self-weight

4.1.1.1.1 Creep, Shrinkage and Relaxation of Prestressed Tendons

The prestressed losses due to creep, shrinkage, and relaxation can be calculated as (AASHTO, 2012):

$$\Delta f_{pLT} = 10 \cdot \frac{f_{pi} \cdot A_{ps}}{A_g} \cdot \gamma_s \cdot \gamma_{st} \cdot 12 \cdot \gamma_h \cdot \gamma_{st} + \Delta f_{pR} \quad (5)$$

The value obtained from the previous equation is just an approximation. According to Section C5.9.5.3 (AASHTO, 2012) the values obtained are conservative; therefore, Article 5.9.5.4 (AASHTO, 2012) can be used instead to obtain these values. However, this article just specifies losses from the time to transfer the girder to when the deck is placed and the time from when the deck is placed until the final time, so for the calculation of prestress losses after release it is used article 5.4.3.2 (AASHTO, 2012).

4.1.1.2 Creep

The creep coefficient can be calculated as follows (AASHTO, 2012):

$$\Psi(t,t_i) = 1.9 \cdot k_s \cdot k_{hc} \cdot k_f \cdot\cdot k_f \cdot t_i{}^{-0.118} \tag{6}$$

Where (AASHTO, 2012);

$$k_s = 1.45 - 0.13\left(\frac{V}{S}\right) \geq 1 \tag{7}$$

Where; $\frac{V}{S}$ is the volume-to-surface ratio and k_{hc} can be defined as (AASHTO, 2012):

$$k_{hc} = 1.56 - 0.008H \tag{8}$$

Where; H is the relative humidity (%).

To calculate the coefficient k_f (AASTHO 2012):

$$k_f = \frac{5}{1+f'_{ci}} \tag{9}$$

To calculate the coefficient k_{td} (AASTHO 2012)

$$k_{td} = \frac{t}{61-4f'_{ci}+t} \tag{10}$$

Where; t is the maturity of concrete (day). Additional equations can be defined as (AASHTO, 2012):

$$\varepsilon_{ci} = \frac{f_{pbt} \cdot A_{ps}}{A_g \cdot E_{ci}} \tag{11}$$

$$\varepsilon_c = \Psi \cdot \varepsilon_{ci} \tag{12}$$

Therefore the losses due to creep (AASTHO 2012):

$$\Delta f_{ps}(CR) = \varepsilon_c \cdot E_p \tag{13}$$

4.1.1.3 Shrinkage

The shrinkage can be calculated as (AASTHO 2012):

$$\varepsilon_{sh} = k_s k_{hc} k_f k_{td} 0.48 \cdot 10^{-3} \tag{14}$$

Where (AASTHO 2012):

$$k_{hs} = 2 - 0.014H \tag{15}$$

Therefore, the total losses due to shrinkage are computed as follows:

$$\Delta f_{ps}(SH) = \varepsilon_{sh} \cdot E_{ps} \tag{16}$$

4.1.1.4 Relaxation of Prestressing Steel

The relaxation of the prestressing steel can be defined as (AASTHO 2012):

$$f_{ps}(t) = f_{pbt}\left[1 - \frac{\log_{10}(t)}{K}\left(\frac{f_{pbt}}{f_{py}} - 0.55\right)\right] \tag{15}$$

Where; K = 30 for low relaxation strands, t is duration of loading in hours (AASTHO 2012):

$$\Delta f_{ps}(RL) = f_{pbt} - f_{ps}(t) \tag{16}$$

4.1.2 Total prestress after all losses have occurred at release

The total prestress after all losses have occurred at release can be calculated as (AASHTO, 2012):

$$f_{pe}(at\ release) = f_{pbt} - \Delta f_{pES} - \Delta f_{ps}(CR) - \Delta f_{ps}(SH) - \Delta f_{ps}(RL) \tag{17}$$

4.2 Stress in Prestressing Steel at Nominal Flexural Resistance (AASTHO 5.7.3.1)

For flanged sections subjected to flexure about one axis where the approximate stress distribution may be considered satisfied by an equivalent rectangular compressive stress block of $0.85 \cdot f'_c$ for which f_{pe} is not less than 0.5 f_{pu}, the average stress in prestressing steel f_{ps} (AASHTO, 2012), may be taken as:

$$f_{ps} = f_{pu}\left(1 - k\frac{c}{d_p}\right) \tag{18}$$

$$k = 2\left(1.04 - \frac{f_{py}}{f_{pu}}\right) \tag{19}$$

To calculate c, the distance from extreme compression fiber to the centroid of the prestressing tendons, (AASHTO, 2012) differentiate for components with just bonded strands or components with both bonded and unbounded strands. For the girders with harped strands the following equation was used (AASTHO 2012)::

$$c = \frac{A_{ps}f_{pu+}A_s f_{s+}A'_s f'_s - 0.85f'_c(b-b_w)h_f}{0.85f'_c\beta_1 b_w + kA_{ps}\frac{f_{pu}}{d_p}} \tag{20}$$

Where; A_{ps} is the area of prestressing steel (in^2), A_s is the area of mild tension reinforcement (in^2), A'_s is the area of compression reinforcement (in^2), b is the width of the compression face of the member (in), b_w is the width of the web, h_f is the depth of compression flange (in) and β_1 is the stress block factor defined in section 5.7.2.2 (AASHTO, 2012). For the purpose of this study, the area of mil tension and compression reinforcement are ignored.

For the girder with debonded tendons, (AASHTO, 2012) has a conservative simplified analysis for components with bonded tendons and with unbonded tendos. Therefore this analysis is used for the girders with debonded strands (AASTHO 2012):.

$$c = \frac{A_{psb}f_{pu+}A_{psu}f_{pe+}A_s f_{s+}A'_s f'_s - 0.85f'_c(b-b_w)h_f}{0.85f'_c\beta_1 b_w + kA_{ps}\frac{f_{pu}}{d_p}} \tag{21}$$

Where; A_{psb} is the area of bonded prestressing steel (in^2), A_{psu} is the area of unbonded prestressing steel (in^2),

4.3 Transfer and development length

The distance where the strand prestressing force is gradually transferred from the steel to the concrete is called transfer length. (AASHTO, 2012) assumes that it varies linearly from zero (at the location where bonding commences) to the effective prestress in the strands after loses at the end of the transfer length. This relationship is reflected in Figure 4.1. Generally, it is assumed for the girder design that this transfer length is equal to 60 times the strand diameter. Some of the factors that influence the transfer length are:

- The method of transfer,
- The concrete strength, and
- The type of the strand.

To develop the strength of the strands, the strand stress needs to be increased from the effective stress in the prestressing steel after losses to the stress in the strand at nominal resistance of the member (AASHTO, 2012).

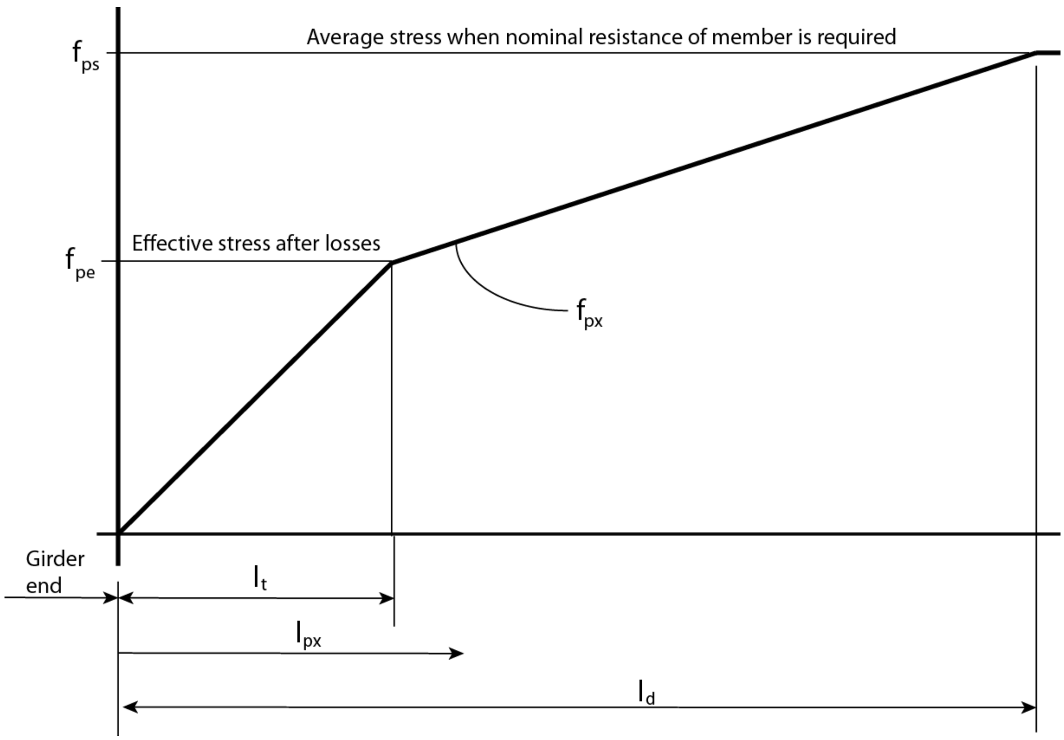

Figure 4.1: Idealized relationship between steel stress and distance from end of girder.

For the development length, (AASHTO, 2012) differentiates between bonded strands and partially bonded strands.

- Bonded Strands Section 5.11.4.2 (AASHTO, 2012):

$$l_d \geq k\left(f_{ps} - \frac{2}{3} f_{pe}\right) d_b \tag{22}$$

Where; d_b is the nominal strand diameter (inch), f_{ps} is the average stress in prestressing steel at the time for which the nominal resistance of the member is required (ksi), and f_{pe} is the effective stress in the prestressing steel after losses, see 4.1. Additionally, k is set to a value of 1.6 for pretensioned members with a depth greater than 24 inches. The variation of strain that was observed in the testing, can be calculated as follows:

- From the beginning of the girder until the end of transfer length (AASHTO, 2012):

$$f_{px} = \frac{f_{pe} l_{px}}{60 d_b} \tag{23}$$

- From the end of transfer length to the end of development length (AASHTO, 2012):

$$f_{px} = f_{pe} + \frac{l_{px} - 60 d_b}{l_d - 60 d_b}\left(f_{ps} - f_{pe}\right) \tag{24}$$

Where; l_{px} is the distance from free end of pretensioned strand to section of girder (inches), and f_{ps} is the design stress in pretensioned strand at nominal flexural strength at the girder (ksi), see 4.1.

- Partially debonded Strands Section 5.11.4.3 (AASHTO, 2012):

$$l_d \geq 2\left(f_{ps} - \frac{2}{3} f_{pe}\right) d_b \tag{25}$$

Partially debonded strands has some limitations imposed by (AASHTO, 2012)

- The number of debonded strands have to be less than 25 percent of the total strands. (AASHTO, 2012)
- The number of debonded strands in a row cannot be more than 40 percent of the total strands in that row. (AASHTO, 2012)
- The debonded strands have to be equally distributed about the centerline of the girder, in such way that the lengths are symmetrically. (AASHTO, 2012)
- Exterior strands in each row have to be fully boded. (AASHTO, 2012)

Chapter 5

Finite Element Model

5.1 Background

The primary objective of finite element (FE) simulation for this research is to establish a valid simulation of the prestress transfer that is produced during the release of the stress from the strands in each type of girder.

Most of the FE models established previously by researchers have not been able to accurately simulate this transfer with a 3D model for large girders. Kahl and Burgueno (2011) modeled a small scale girder with 3D model for the girder geometry and for the strands. Since they were able to consider the strand as a 3D element, introducing an initial stress in the element allowed for the prestress transfer at the end of the girder to occur (Kahl and Burgueno, 2011). This approach was followed at the beginning of this study, but the computational cost of the strands transferring the stress was greater than the capabilities of the computer. A similar study was conducted by Oliva and Okumus (2011), which modeled a wide flange girder, similar to the one in this study; however, modeling the strands was conducted by placing voids in the location of the strands and then manually applying the prestressing forces.

5.2 Materials

5.2.1 Concrete

During the release of the strands, other researchers have seen the appearance of microcracks at the end of the girder (Kahl and Burueno, 2011; Oliva and Okumus, 2011). Therefore, the concrete damage plasticity model has been used to characterize the cracks in the FEM model (Kahl and Burueno, 2011; Oliva and Okumus, 2011). This model represents the concrete as an inelastic material, combining concepts of isotropic damaged elasticity with isotropic tensile and compressive plasticity. However, during the testing in this study, cracks have not appeared during the monitoring period of the Therefore, concrete is assumed as only a linear elastic material for the release. The modulus of elasticity used are the same ones as the ones discussed in Chapter 4.

5.2.2 Strands

The modulus of elasticity varied between both prestressing methods; for the harped strands the modulus of elasticity was 28,600 ksi, and for the girder with debonded strands, the modulus of elasticity was 28,500 ksi. Contrarily, the Poisson's ratio was assumed to be 0.3 for both cases.

5.3 Element Types

To capture the effect of release, three dimensional tetrahedral elements (C3D4 in Abaqus library [Figure 5.1 and Figure 5.2]) was used to model the girder. The strands were modeled as a 3D truss dimensional (T3D2 in Abaqus library [Figure 5.3 and Figure 5.4]), since it was not computationally feasible to model these strands as a solid continuum-type element (ideal model). For the harped strands, the nominal diameter was 0.5 inches and the cross sectional area applied was 0.153 in^2. The girders with debonded strands had a nominal diameter 0.6 inches and the cross sectional of 0.216 in^2.

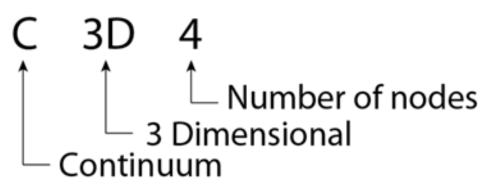

Figure 5.1: Abaqus library naming.

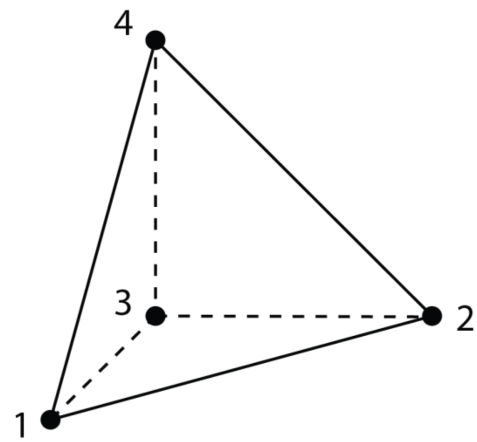

Figure 5.2: 4-node tetrahedral element.

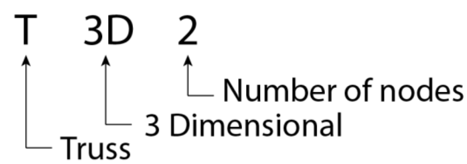

Figure 5.3: Abaqus library naming.

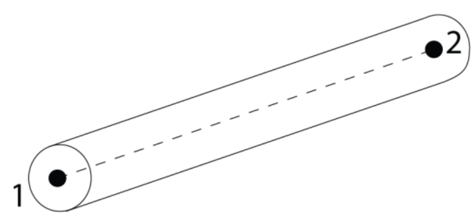

Figure 5.4: 2-node 3 dimensional truss element.

5.3.1 Concrete

To simulate the concrete, a three dimensional tetrahedral elements (C3D4 from the Abaqus library) was utilized. Due to the dimension of the girder and the geometry, an automated mesh technique was used. For this type of technique, the most accurate elements to fill all the arbitrary shapes are the tetrahedral elements.

5.3.2 Strands

As previously stated, Oliva and Okumus (2011) modeled the debonded bonded strands as holes; therefore the generated mesh was irregular. This technique was attempted in this study but caused resulted irregular mesh. Therefore, no strands were modeled in the debonded area.

The strands were created with chained wires as three dimensional trusses (T3D2 in the Abaqus Element Library), defining the different points that were needed to applied the forces in order to model each strand. Figure 5.5, Figure 5.6 and Figure 5.7 shows different views for the girder with harped strands and with debonded strands.

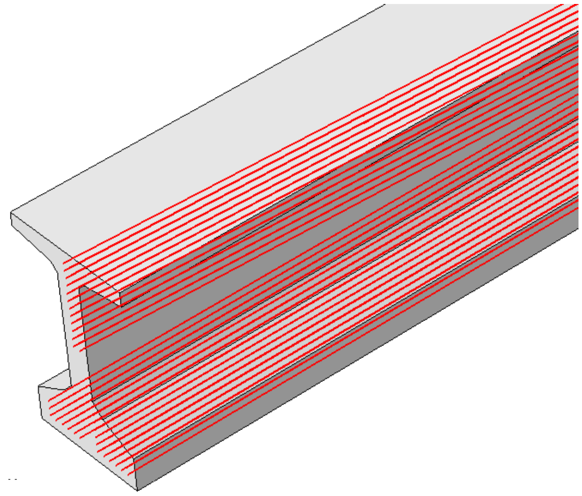

Figure 5.5: End view of girder with harped strands.

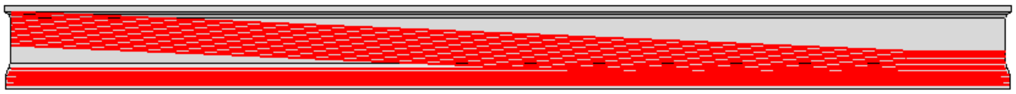

Figure 5.6: Elevation view of girder with harped strands.

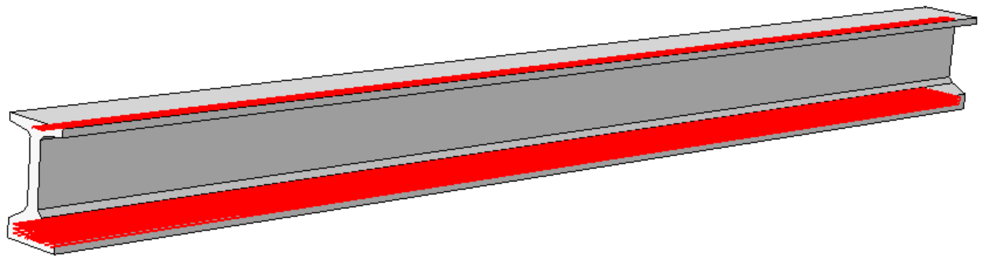

Figure 5.7: View of girder with debonded strands.

5.4 Constraints

The constrain feature was utilized to ensure that the strands are embedded into the concrete. The whole model of the girder was defined as the host region and the strands are the embedded elements. Additionally, utilizing this feature in Abaqus ensures that the strands do not incorrectly translate into the concrete when forces are applied.

5.5 Boundary Conditions

Symmetry of the girder about the midspan and the forces applied allows the girder to be modeled as only half of the total length. Resulting in a major reduction in the computational cost of the analysis. The rotation and movement along the X and Z direction is restrained at midspan. At the beginning of the girder the only restrain is that the girder cannot move in the Y direction. This will allow the girder to camber up once the concrete is released and it will be supported by the end of the girder.

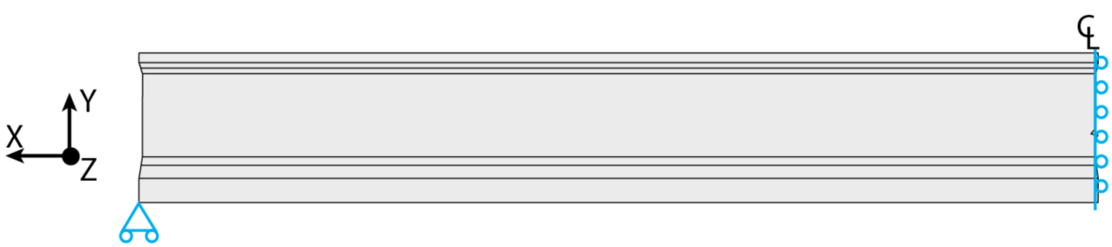

Figure 5.8: Boundary conditions of finite element model.

5.6 Prestress Transfer

The strands cannot be released until the concrete hasn't achieved a minimum compressive strength, which is always specified in the shop drawings of the girders. Section 4.2 provides the equations to calculate the effective stress (f_{px}) along the girder end (l_{px}). The force to be applied at different locations (Figure 5.9 and Figure 5.10) was computed by multiplying the effective stress by the nominal area of the strand. The concrete stresses are zero at the girder end, and in order to simulate the real contribution of the steel, it has been considered a linear reduction of the cross sectional area from the end of the girder until the end of the development length where all the nominal area of the steel has been considered.

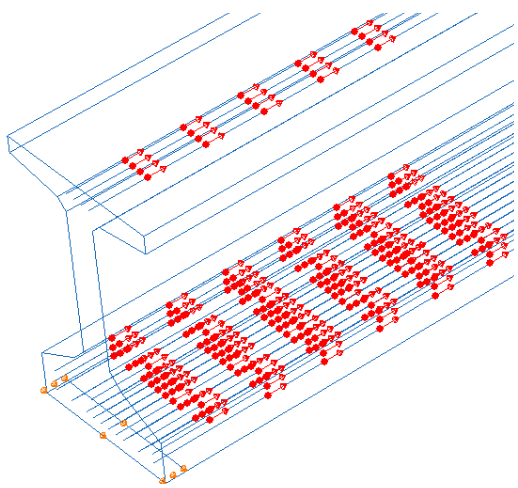

Figure 5.9: Prestress force at different locations for girder with debonded strands.

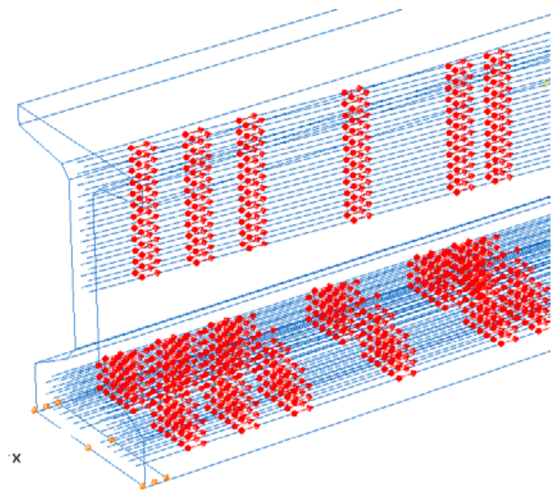

Figure 5.10: Prestress force at different locations for girder with harped strands.

5.7 Mesh

The entire element is meshed to define the location of the nodes where forces and displacements are calculated. Therefore, finer meshes lead to more accurate results but results in a greater computational time. It is beneficial to balance the size of the element with the computational time. Figure 5.11 and Figure 5.12 shows the result of meshing the girder in both cases.

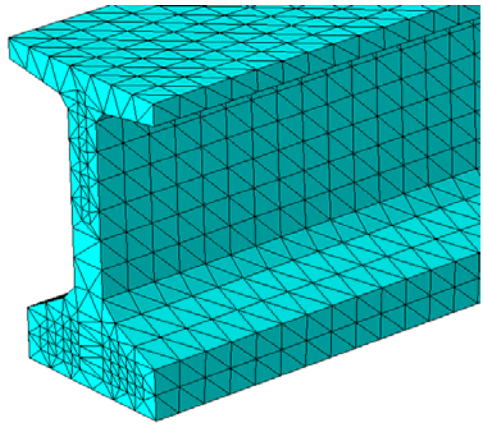

Figure 5.11: End view of mesh at girder with harped strands.

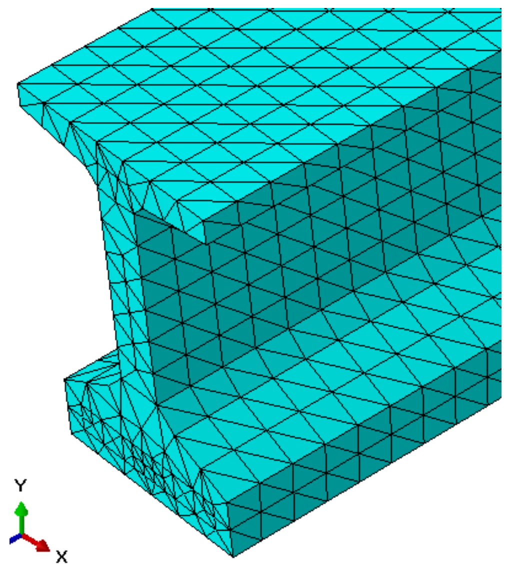

Figure 5.12: End view of mesh at girder with debonded strands.

5.8 Results and Comparison

5.8.1 Harped Strands

The results obtained from the Abaqus harped strand girder model showed the transfer of the prestress along the length of the girder (Figure 5.13). A comparison of strain results between second and third monitoring and the Abaqus results is provided in Figure 5.14. It should be noted that the general trend of the field measurements can be modeled in Abaqus for the strains measure at the bottom of the girder. However, the tensile and compressive forces observed at the very end of the girder during monitoring was not obtained with the Abaqus model.

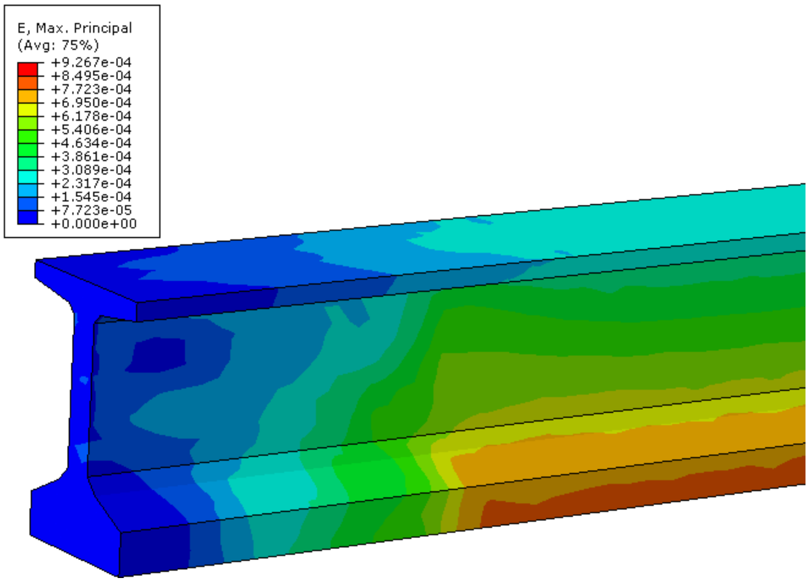

Figure 5.13: Results obtained from Abaqus for girder with harped strands.

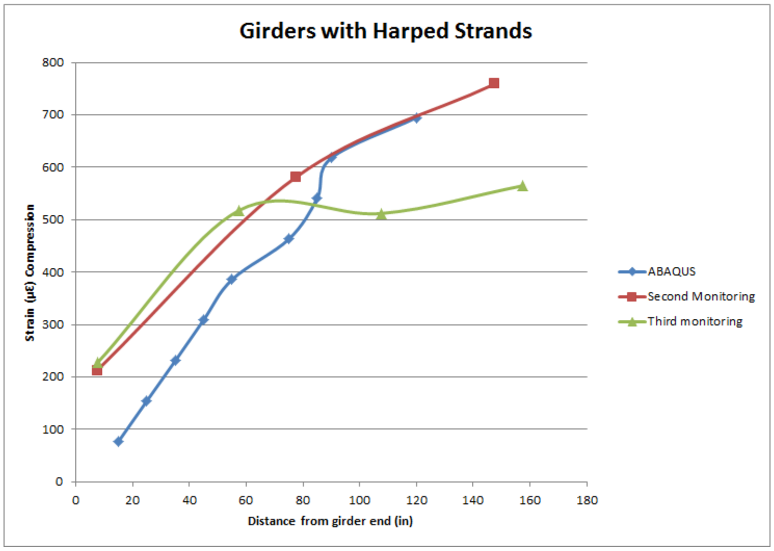

Figure 5.14: Comparison of Abaqus results with testing measurements for the harped strands.

5.8.2 Debonded Strands

The strain results obtained from the Abaqus model for the debonded strand girder are provided in Figure 5.15, and a comparison between the Abaqus results and second and third monitoring are shown in

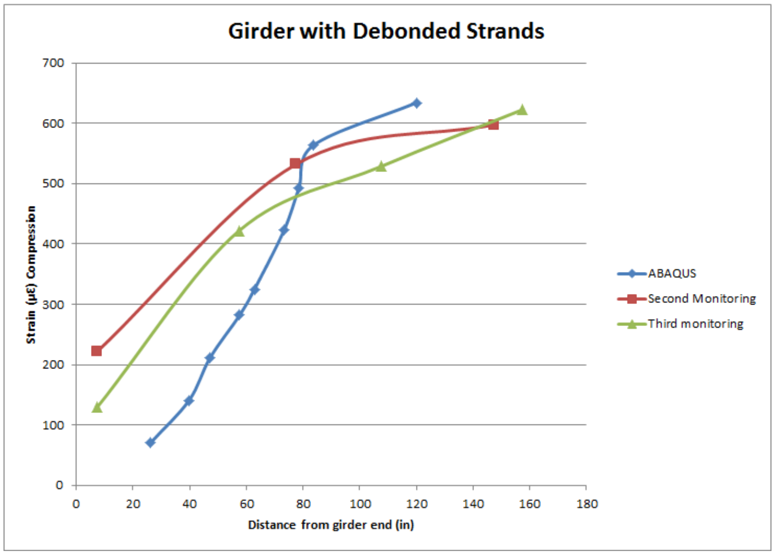

Figure 5.16. In general, lower strain values were obtained from the Abaqus results; however, the values obtained at the center of the web at the end of the Abaqus modeled girder are greater than those measured during the monitoring. The strains obtained at the bottom of the girder along the girder length follows the general trend of the monitoring results.

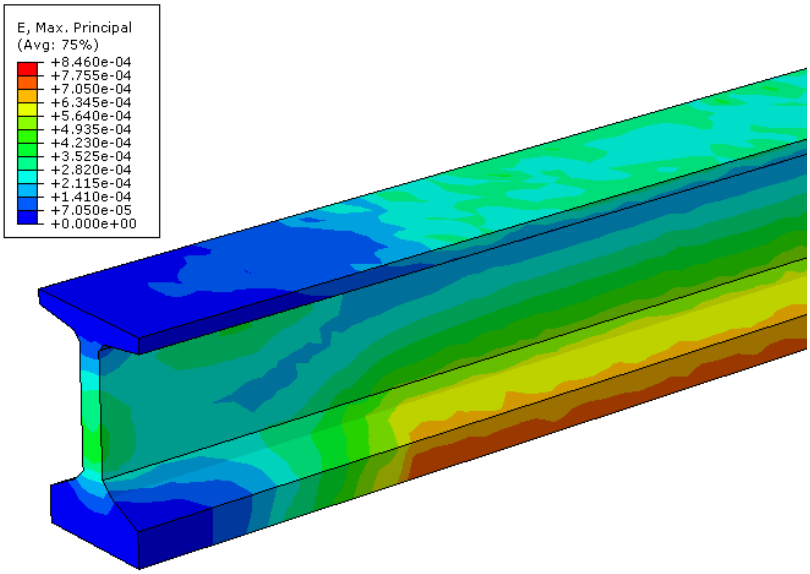

Figure 5.15: Results obtained from Abaqus for girder with debonded strands.

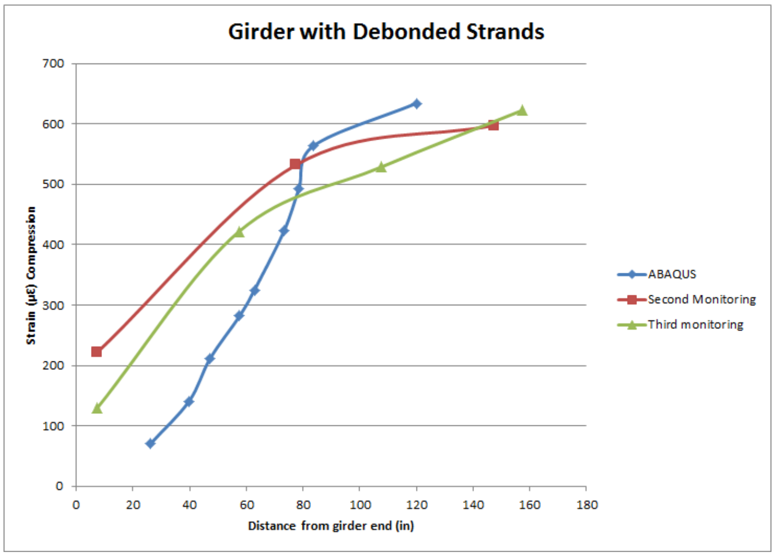

Figure 5.16: Comparison of Abaqus results with testing measurements for the debonded strands.

Chapter 6

General Results and Conclusions

The following conclusions can be drawn from the strain gauging monitoring and Abaqus modeling conducted in this study for Tx54 girders with either the debonded and harped strands:

1. Flame cutting of the strands led to abrupt strain change in the strain gauges at the end of the debonded girders.
2. Section near the end of the girders of both types of prestressed girders experienced both tension and compression along the same section.
3. Strains at the end of the girders with harped strands showed higher values that in the girders with debonded strands.
4. The construction process of the girders with debonded strands is safer than that of girders with harped strands, because the hold-down and hold-up anchors are not required during the construction process.
5. Assembling the reinforcement cages for the girder with the debonded strands is less time-consuming and requires less labor work because it can be prefabricated before being placed in the prestressing bed.
6. The need for concrete blocks at the ends of the prestressing bed for harped strands is time-consuming since those blocks weights about 18,500 lbs and the work requires a forklift to place the blocks on top of the girders. Additionally, this could cause damage to the girders if care is not taken during the placement.
7. Microcracks were still observed in both types of girders.

Appendix A

I-Girder Standard by Texas Department of Transportation

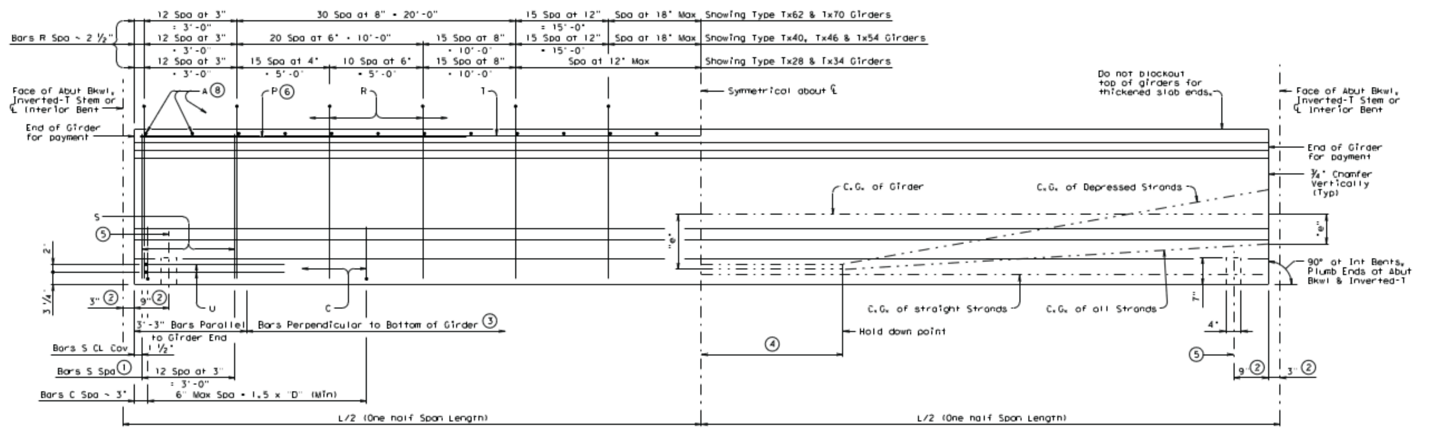

GIRDER ELEVATION

1. Bundle with Bars R.
2. Measured along ℄ Girder at Interior Bents; perpendicular to Abutment Bkwl or Inverted-T Stem.
3. The average of the top and bottom spacing of Bars R cannot exceed the required spacing.
4. L/20, but not less than 5'-0" (-0,+2').
5. ℄ 4" x 1 ½" Vertical Slotted Hole at doweled girder end [labeled (D) on Bridge Layout]. Required for outside girder only or as shown on substructure details. Anchorage holes may be tapered (4 ¾" x 1 ⅝") at base. If holes are formed with sheet metal, forms may be left in place.
6. Bars P (#6 x 15'-0") are only required when "e" at girder ends exceeds 0.25 x "D". At the fabricator's option bars larger than #6 may be used. When L is less than 50 ft, Bars P are to be the same length as Bars T.
7. 1 ⅜" Clear Cover to Bars S.
8. Space Bars A at 6" Max for girders requiring overhang bracket hangers. Space at 12" Max for all other girders. Tie to Bars R as necessary. See standard IGMS for "Deck Forming Notes".

GIRDER DIMENSIONS AND SECTION PROPERTIES

Girder Type	"D" (in.)	"B" (in.)	"Yt" (in.)	"Yb" (in.)	Area (in.²)	"Ix" (in.⁴)	"Iy" (in.⁴)	Weight (plf)
Tx28	28	6	15.02	12.98	585	52,772	40,559	610
Tx34	34	12	18.49	15.51	627	88,355	40,731	653
Tx40	40	18	21.90	18.10	669	134,990	40,902	697
Tx46	46	22	25.90	20.10	761	198,089	46,478	793
Tx54	54	30	30.49	23.51	817	299,740	46,707	851
Tx62	62	37 ½"	33.72	28.28	910	463,072	57,351	948
Tx70	70	45 ½"	38.09	31.91	966	628,747	57,579	1,006

GENERAL NOTES:

Designed in accordance with AASHTO LRFD Specifications.

All concrete must be Class H. Provide Class H(HPC) if shown elsewhere in plans.

All reinforcing bars must be Grade 60.

An equal area of deformed Welded Wire Reinforcement (WWR) (ASTM A497) may be substituted for Bars A, C, R or T unless otherwise noted.

It is permissible for bars or strands to come in contact with materials used in forming anchor holes.

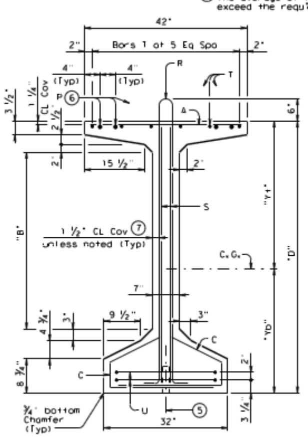

TYPE Tx62 & Tx70

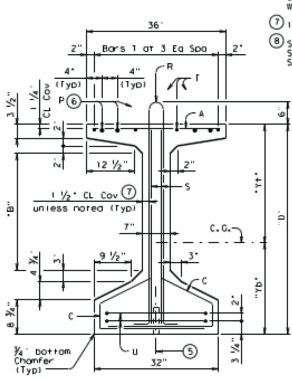

TYPE Tx46 & Tx54

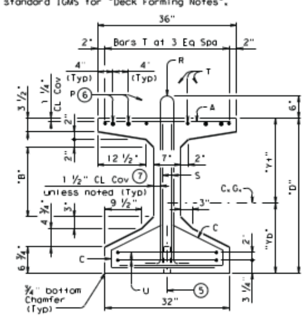

TYPE Tx28, Tx34 & Tx40

HL93 LOADING SHEET 1 OF 2

Texas Department of Transportation
Bridge Division

PRESTRESSED CONCRETE I-GIRDER DETAILS

IGD

FILE: igdstdel.dgn	DN: TxDOT	CK: JMH	DW: JTR	CK: JMH
© TxDOT June 2007	DISTRICT	FEDERAL AID PROJECT		SHEET
REVISIONS 02/09 General Notes. 12/10 Optional Top Flange Reinforcing.	COUNTY	CONTROL	SECT	JOB / HIGHWAY

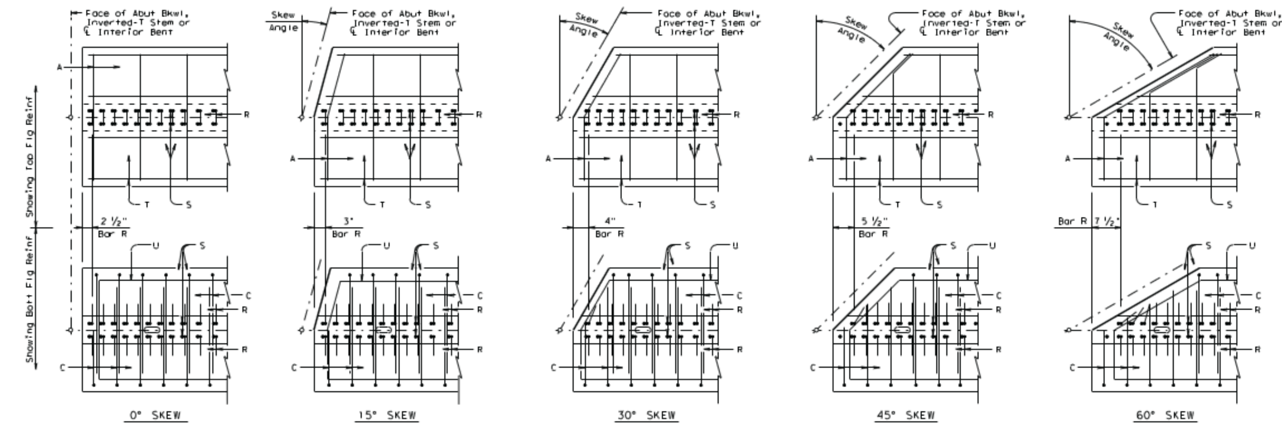

0° SKEW

15° SKEW

30° SKEW

45° SKEW

60° SKEW

PLAN OF GIRDER ENDS ⑨

To control top flange cracking that may occur during form removal, additional top flange reinforcing may be placed as shown in girder ends at the Fabricator's option.

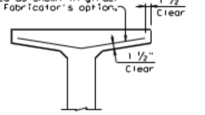

OPTIONAL TOP FLANGE REINFORCING DETAIL

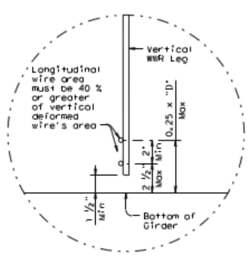

OPTIONAL WELDED WIRE REINFORCEMENT (WWR) DETAIL

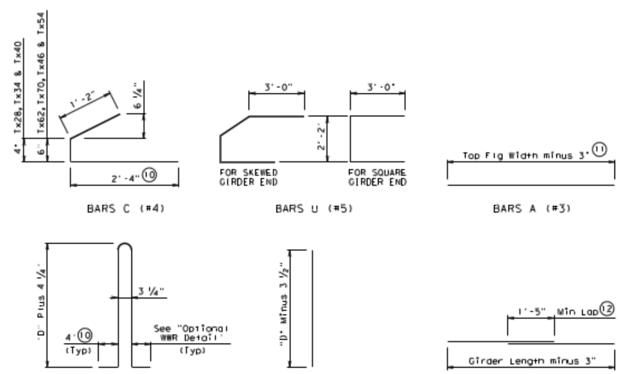

BARS C (#4)

BARS U (#5)

BARS A (#3)

BARS R (#4) ⑬

BARS S (#6)

BARS T (#4)

⑨ Reinforcing patterns shown are provided as guides to determine reinforcement placement in skewed ends. Place Bars S as close to girder end as cover requirements permit, which may prevent them to be bundled with Bars R.

⑩ Bars may be cut or bent at skewed end as required.

⑪ Increase as necessary for bars at skewed end.

⑫ No portion of bar less than 10 ft.

⑬ For Welded Wire Reinforcement (WWR) option, area of Bars R may be reduced in proportion to the increase in reinforcement yield strength over 60 ksi. Yield strength of WWR is limited to 75 ksi.

HL93 LOADING

SHEET 2 OF 2

Texas Department of Transportation
Bridge Division

PRESTRESSED CONCRETE I-GIRDER DETAILS

IGD

FILE: Igdstde1.dgn	DN: TxDOT	CK: JMH	DW: JTR	CK: JMH
©TxDOT June 2007	DISTRICT	FEDERAL AID PROJECT		SHEET
REVISIONS 02/09 General Notes. 12/10 Optional Top Flange Reinforcing.	COUNTY	CONTROL	SECT / JOB	HIGHWAY

LEVELS DISPLAYED
PATH:

DESIGNED GIRDERS (DEPRESSED STRANDS)

STRUCTURE	SPAN NO.	GIRDER NO.	GIRDER TYPE	PRESTRESSING STRANDS								CONCRETE	
				NON-STD STRAND PATTERN	TOTAL NO.	SIZE (in)	STRGTH fpu (ksi)	"e" ℄ (in)	"e" END (in)	DEPRESSED NO.	DEPRESSED TO (in)	RELEASE STRGTH ① f'ci (ksi)	MINIMUM 28 DAY COMP STRGTH f'c (ksi)

OPTIONAL DESIGN

DESIGN LOAD COMP STRESS (TOP ℄) (SERVICE I) fct (ksi)	DESIGN LOAD TENSILE STRESS (BOTT ℄) (SERVICE III) fcb (ksi)	REQUIRED MINIMUM ULTIMATE MOMENT CAPACITY (STRENGTH I) (ft-kips)	LIVE LOAD DISTRIBUTION FACTOR ②	
			Moment	Shear

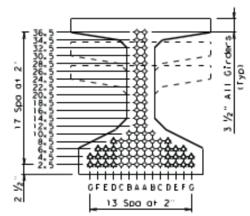

TYPE Tx28, Tx34 & Tx40③

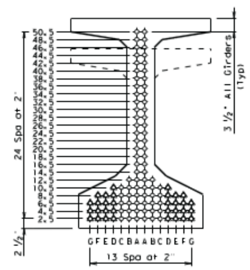

TYPE Tx46 & Tx54③

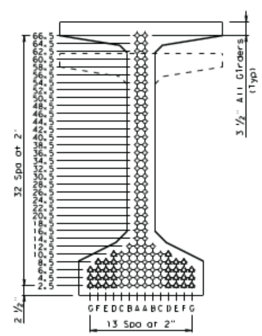

TYPE Tx62 & Tx70③

NON-STANDARD STRAND PATTERNS

PATTERN	STRAND ARRANGEMENT AT ℄ OF GIRDER

GENERAL NOTES:

Designed in accordance with AASHTO LRFD Specifications.

All concrete must be Class H. Provide Class H(HPC) if shown elsewhere in plans. All reinforcing bars must be Grade 60.

When shown on this sheet, the Fabricator has the option of furnishing either the designed depressed strand girder or an approved optional design. All optional design submittals must be signed, sealed and dated by a registered Professional Engineer.

Optional designs for girders 120 feet or longer must have a calculated residual camber equal to or greater than that of the designed girder.

Prestress losses for the designed girders have been calculated for a relative humidity of percent. Optional designs must likewise conform.

For depressed strand designed girders, strands must be located as low as possible on the 2" grid system unless a Non-Standard Strand Pattern is indicated. Fill row "2.5", then row "4.5", then row "6.5", etc., beginning each row in the "A" position and working outward until the required number of strands is reached. All strands in the "A" position must be depressed, maintaining the 2" spacing so that, at the girder ends, the upper two strands are in the position shown in the table.

Strands for the designed girder must be low relaxation strands pretensioned to 75 percent of fpu each.

Seal cracks in girder ends exceeding 0.005" in width as directed by the Engineer. The fabricator is permitted to decrease the spacing of Bars R and S by providing additional bars to help limit crack width provided the decreased spacing results in no less than 1" clear between bars. The fabricator must take an approved corrective action if cracks greater than 0.005" form on a repetitive basis.

① Based on the following allowable stresses (ksi):

Compression = 0.65 f'ci

Tension = $0.24\sqrt{f'ci}$

Optional designs must likewise conform.

② Portion of full HL93.

③ Full-length debonded strands are only permitted in strand positions marked Δ. Double wrap full-length debonded strands in outermost position of each row. Full-length debonding must comply with Item 426.4.F.4.

HL93 LOADING

Texas Department of Transportation
Bridge Division

PRESTRESSED CONCRETE I-GIRDER DESIGNS (NON-STANDARD SPANS)

IGND

FILE: Igndste1.dgn	DN: JMH	CK: TxDOT	DW: JTR	CK: TxDOT
©TxDOT June 2007	DISTRICT	FEDERAL AID PROJECT		SHEET
REVISIONS 02/09: General Notes. 10/09: General Notes. 12/10: Rel Strgth & LLDF.	COUNTY	CONTROL	SECT	JOB	HIGHWAY

LEVELS DISPLAYED ACC*

Appendix B

Shop drawings provided by the precast plants

Girder with Harped Strands

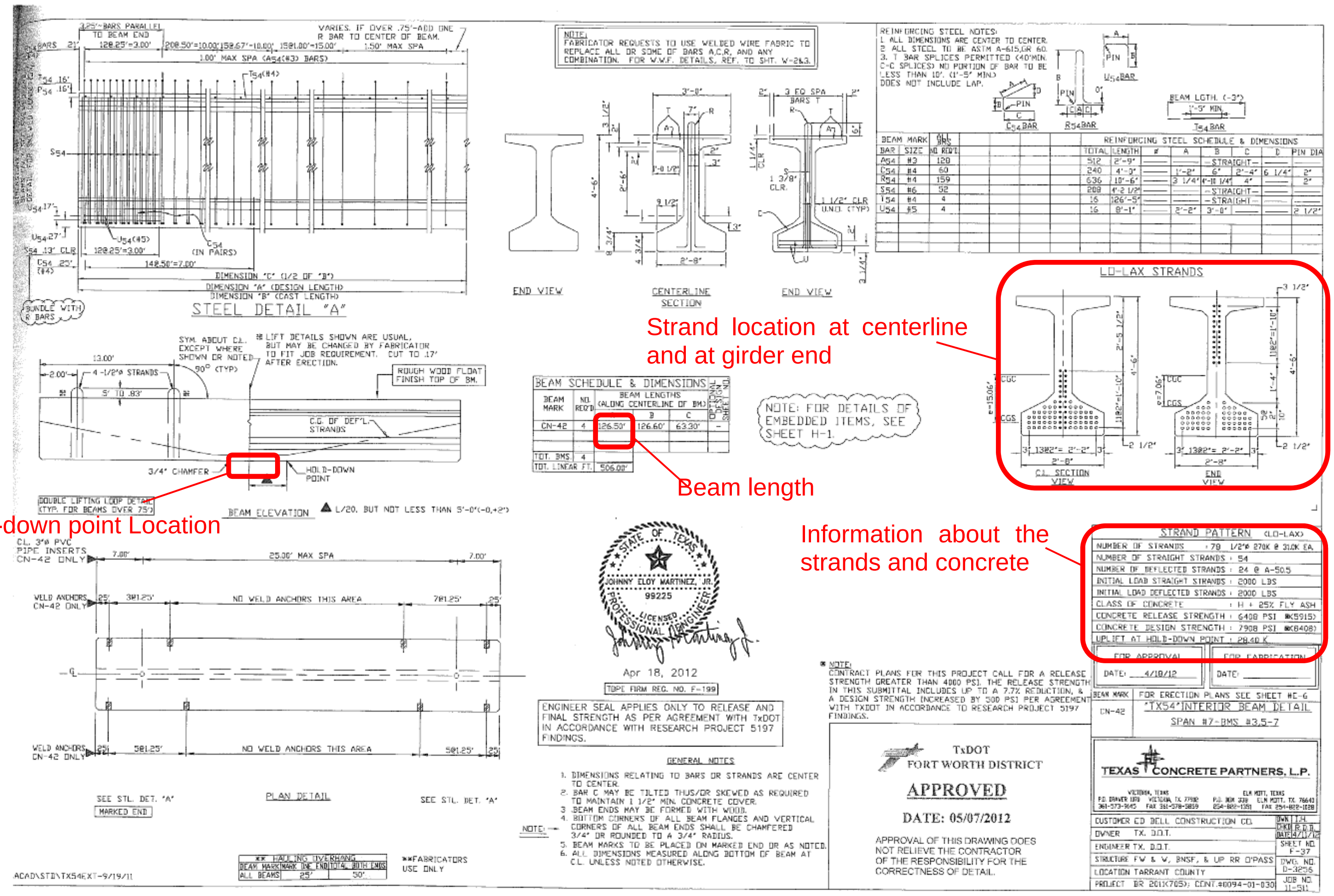

Girder with Debonded Strands

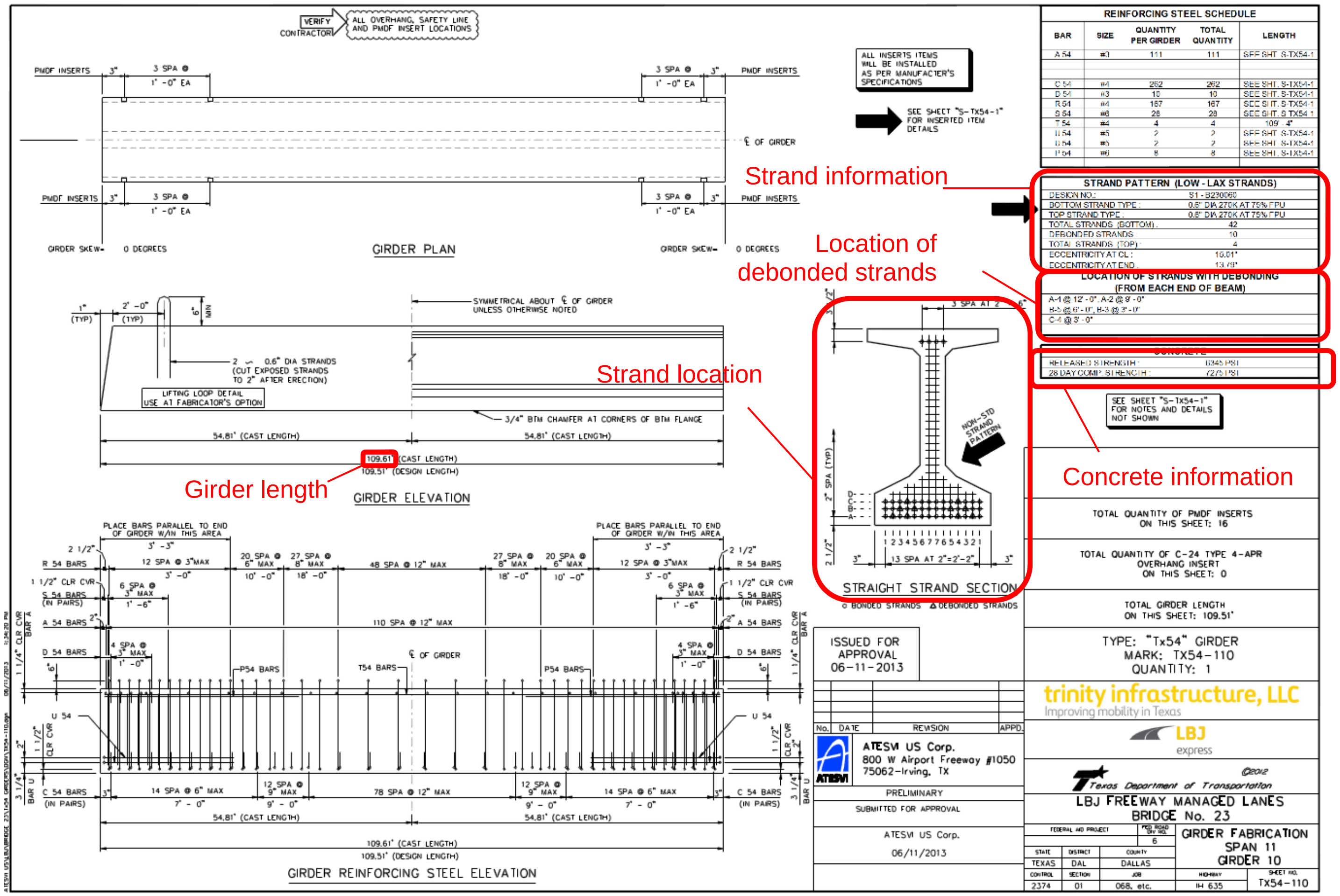

Appendix C

Calculations

Girder with harped strands

From the shop drawings in APENDIX B, the information that it can be obtained is the following:

- Ø strands = 0.5", Nominal area = 0.153 in^2 (Naaman, 2012)
- Total number of strands = 78, $A_{ps} = 78 \cdot 0.153 \text{ in}^2 = 11.93 \text{ in}^2$
- Number of deflected strands = 24
- Tensile strength of prestressing steel (f_{pu}) = 270 ksi
- Type of tendon = low relaxation strand
- Compressive strength of concrete (f'_c) = 7908 psi
- Compressive strength of concrete at release (f'_{ci}) = 6408 psi
- Eccentricity at center line, e_{CL} = 15.06 in
- Eccentricity at end, e_{end} = 7.06 in

With the information of the location of the strands, it can be obtained the distance from extreme compression fiber to the centroid of the prestressing tendons (d_p)

Centerline section:

$$d_p \cdot 72 = 2 \cdot 29.5\ in + 2 \cdot 31.5\ in + 2 \cdot 33.5\ in + 2 \cdot 35.5\ in + 2 \cdot 37.5\ in + 2 \cdot 39.5\ in + 4 \cdot 41.5\ in + 8 \cdot 43.5\ in + 12 \cdot 45.5\ in + 14 \cdot 47.5\ in + 14 \cdot 49.5\ in + 14 \cdot 51.5\ in$$

$$d_p = 49.35\ in$$

End section:

$$d_p \cdot 72 = 2 \cdot 3.5\ in + 2 \cdot 5.5\ in + 2 \cdot 7.5\ in + 2 \cdot 9.5\ in + 2 \cdot 11.5\ in + 2 \cdot 13.5\ in + 2 \cdot 15.5\ in + 2 \cdot 17.5\ in + 2 \cdot 19.5\ in2 + 2 \cdot 21.5\ in + 2 \cdot 23.5\ in + 2 \cdot 25.5\ in + 2 \cdot 41.5\ in + 6 \cdot 43.5\ in + 10 \cdot 45.5\ in + 12 \cdot 47.5\ in + 12 \cdot 49.5\ in + 12 \cdot 51.5\ in$$

$$d_p = 40.32\ in$$

The beam length in this case is 126.5 ft, but for the purpose of this study, this length is going to be considered 110 ft to be able to compare it to the other type of prestressing girders.

Prestress losses (Section 5.9.5.1 (AASHTO, 2012))

As discussed in 4.1, the total losses for a pretensioned member is:

$\Delta f_{pT} = \Delta f_{pES} + \Delta f_{pLT}$ Equation 5.9.5.1-1 (AASHTO, 2012)

Elastic Shortening

$\Delta f_{pES} = \frac{E_P}{E_{ct}} f_{cgp}$ Equation 5.9.5.2.3a-1 (AASHTO, 2012)

According to Comment C5.9.5.2.3a (AASHTO, 2012), the loss due to elastic shortening in pretensioned member may be determined by the following alternative equation:

$$\Delta f_{pES} = \frac{A_{ps} \cdot f_{pbt} \cdot \left(I_g + {e_m}^2 \cdot A_g\right) - e_m \cdot M_g \cdot A_g}{A_{ps} \cdot \left(I_g + {e_m}^2 \cdot A_g\right) + \frac{A_g \cdot I_g \cdot E_{ci}}{E_p}}$$

Where:

A_g is the gross area of section, $A_g = 817\ in^2$

E_{ci} is the modulus of elasticity of concrete at transfer, that it can be obtained with equation 5.4.2.4-1 (AASHTO, 2012):

$E_{ci} = 33{,}000 \cdot K_1 \cdot w_c{}^{1.5}\sqrt{f'_{ci}}$

Where:

K_1 is the correction factor for source of aggregate to be taken as 1.0 unless determined by physical test, and as approved by the authority of jurisdiction (AASHTO, 2012), $K_1 = 1$.

w_c is the unit weight of concrete and according to table 3.5.1-1 (AASHTO, 2012), the unit weight for normal weight concrete with $5 \leq f'_c \leq 15$ ksi is $0.140 + 0.001 \cdot f'_c$, since f'_c is 6.4 ksi, $w_c = 0.1464\ kcf$

Therefore,

$E_{ci} = 4676.44\ ksi$

E_p is the modulus of elasticity of prestressing tendons, $E_p = 28{,}600\ ksi$

$e_{m=}e_{CL}$ is the average prestressing steel eccentricity at midspan, $e_m = 15.06\ in$

f_{pbt} is the stress in prestressing steel immediately prior to transfer. According to table 5.9.3-1 (AASHTO, 2012), for low relaxation strands, the stress limit can be taken as $f_{pbt} = 0.75 \cdot f_{pu} = 0.75 \cdot 270\ ksi = 202.5\ ksi$

I_g is the moment of inertia of the gross concrete section that can be obtained from the standard in Appendix A.

, $I_g = 299{,}740\ in^4$.

$M_g$is the midspan moment due to self-weight of the concrete. The self-weight of the concrete is obtained from the standard in Appendix A

$$M_g = \frac{selfweight \cdot l^2}{8} = \frac{0.851\ klf\ \cdot 110\ ft^2}{8} = 1287.14\ k \cdot ft = 15446\ k \cdot in$$

Therefore,

Δf_{pES}

$$= \frac{11.93\ \text{in}^2 \cdot 202.5\ ksi \cdot (299{,}740\ in^4 + 15.06^2\ in^2 \cdot 817\ in^2) - 15.06\ in \cdot 15446\ k \cdot in \cdot 817\ in^2}{11.93\ \text{in}^2 \cdot (299{,}740\ in^4 + 15.06^2\ in^2 \cdot 817\ in^2) + \frac{817\ in^2 \cdot 299{,}740\ in^4 \cdot 4676.44\ ksi}{28{,}600\ ksi}}$$

$\Delta f_{pES} = 21.43\ ksi$

Creep, Shrinkage and Relaxation of Prestressed Tendons

$\Delta f_{pLT} = 10 \cdot \frac{f_{pi} \cdot A_{ps}}{A_g} \cdot \gamma_s \cdot \gamma_{st} \cdot 12 \cdot \gamma_h \cdot \gamma_{st} + \Delta f_{pR}$ Equation 5.9.5.3-1 (AASHTO, 2012)

The value obtained from equation 5.9.5.3-1 (AASHTO, 2012) is just an approximation. According to Comment C5.9.5.3 (AASHTO, 2012) the values obtained are conservative so article 5.9.5.4 (AASHTO, 2012) can be used instead to obtain these values. However, this article just specifies losses from the time to transfer the girder to when the deck is placed and the time from when the deck is placed until the final time, so for the calculation of prestress losses after release article 5.4.3.2 (AASHTO, 2012) is used.

Creep

Creep coefficient:

$\Psi(t, t_i) = 1.9 \cdot k_s \cdot k_{hc} \cdot k_f \cdot k_{td} \cdot t_i^{-0.118}$ Equation 5.4.2.3.2-1 (AASHTO, 2012)

Where:

$k_s = 1.45 - 0.13\left(\frac{V}{S}\right) \geq 1$ Equation 5.4.2.3.2-2 (AASHTO, 2012)

$\frac{V}{S}$ is the volume-to-surface ratio, $\frac{V}{S} = 0.85$

$k_s = 1.34 \geq 1$ OK

$k_{hc} = 1.56 - 0.008H$ Equation 5.4.2.3.2-3 (AASHTO, 2012)

H is the relative humidity (%), $H = 65$

k_{hc}= 1.04

$k_f = \dfrac{5}{1 + f'_{ci}}$ Equation 5.4.2.3.2-4 (AASHTO, 2012)

$k_f = 0.67$

$k_{td} = \dfrac{t}{61 - 4f'_{ci} + t}$ Equation 5.4.2.3.2-5 (AASHTO, 2012)

t is the maturity of concrete (day), it is taken as 1 since that is the time that takes from the moment the concrete is pour to when the strands are released.

$$k_{td} = \frac{1}{61 - 4 \cdot 6408\, psi + 1} = 0.027$$

Therefore,

$$\Psi = 1.9 \cdot 1.34 \cdot 1.04 \cdot 0.67 \cdot 0.027 \cdot 1^{-0.118} = 0.05$$

$$\varepsilon_{ci} = \frac{f_{pbt} \cdot A_{ps}}{A_g \cdot E_{ci}} = \frac{202.5\, ksi \cdot 11.93\, in^2}{817\, in^2 \cdot 4676.44\ \ ksi} = 0.000632$$ (Naaman, 2012)

$$\varepsilon_c = \Psi \cdot \varepsilon_{ci}$$

$\varepsilon_c = 3.16 \cdot 10^{-5}$

$$\Delta f_{ps}(CR) = \varepsilon_c \cdot E_p = 0.9\, ksi$$

Shrinkage

$\varepsilon_{sh} = k_s k_{hc} k_f k_{td} 0.48 \cdot 10^{-3}$ Equation 5.4.2.3.3-1 (AASHTO, 2012)

In which:

$k_{hs} = 2 - 0.014H = 1.09$ Equation 5.4.2.3.3-2 (AASHTO, 2012)

$\varepsilon_{sh} = 1.3 \cdot 10^{-5}$

$\Delta f_{ps}(SH) = \varepsilon_{sh} \cdot E_p = 1.3 \cdot 10^{-5} \cdot 28{,}600\, ksi = 0.37\, ksi$

Relaxation of Prestressing Steel

$$f_{ps}(t) = f_{pbt}\left[1 - \frac{\log_{10}(t)}{K}\left(\frac{f_{pbt}}{f_{py}} - 0.55\right)\right]$$

Where:

$K = 30$ for low relaxation strands

t is duration of loading in hours. $t = 24\ h$ since it is when the strands are released.

f_{py} is the yield strength of prestressing steel (ksi)

From table C5.7.3.1.1-1 (AASHTO, 2012), for a low lax strand:

$$f_{py} = 0.9 \cdot f_{pu} = 0.9 \cdot 270\ ksi = 243\ ksi$$

Therefore,

$$f_{ps}(t) = 202.5\ ksi\left[1 - \frac{\log_{10}(24\ h)}{30}\left(\frac{202.5\ ksi}{243\ ksi} - 0.55\right)\right] = 199.86\ ksi$$

$$\Delta f_{ps}(RL) = f_{pbt} - f_{ps}(t) = 202.5\ ksi - 199.86\ ksi = 2.64\ ksi$$

Total Prestress losses at release

$$f_{pe}(at\ release) = f_{pbt} - \Delta f_{pES} - \Delta f_{ps}(CR) - \Delta f_{ps}(SH) - \Delta f_{ps}(RL)$$

$$f_{pe}(at\ release) = 202.5 - 21.43\ ksi - 0.9\ ksi - 0.37\ ksi - 2.64\ ksi = 177.16\ ksi$$

Stress in Prestressing Steel at Nominal Flexural Resistance, section 5.7.3.1 (AASHTO, 2012).

As explained in 4.1.1.4, the average stress in prestressing steel (f_{ps}) may be taken as:

$$f_{ps} = f_{pu}\left(1 - k\frac{c}{d_p}\right) \qquad \text{Equation 5.7.3.1.1-2 (AASHTO, 2012)}$$

Where:

$$k = 2\left(1.04 - \frac{f_{py}}{f_{pu}}\right) \qquad \text{Equation 5.7.3.1.1-1 (AASHTO, 2012)}$$

To calculate c, the distance from extreme compression fiber to the centroid of the prestressing tendons:

$$c = \frac{A_{ps} f_{pu+} A_s f_{s+} A'_s f'_s - 0.85 f'_c (b - b_w) h_f}{0.85 f'_c \beta_1 b_w + k A_{ps} \frac{f_{pu}}{d_p}}$$ Equation 5.7.3.1.1-3 (AASHTO, 2012)

ß$_1$ is the stress block factor defined in section 5.7.2.2 (AASHTO, 2012). Since f'_c is 7.9 ksi, interpolating $\beta_1 = 0.655$

The value of k can be obtained directly from table C5.7.3.1.1-1 (AASHTO, 2012). For low lax strand, $k = 0.28$

Since the girders texted are Tx54 the following properties are obtained from the bridge standards from Texas Department of Transportation are shown in Appendix A.

$b = 36\ in$, $b_w = 7\ in$, $h_f = 7.5\ in$.

Therefore:

$$c = \frac{11.93\ \text{in}^2 \cdot 270\ ksi - 0.85 \cdot 7.9\ ksi(36\ in - 7\ in)7.5\ in}{0.85 \cdot 7.9\ ksi \cdot 0.655 \cdot 7\ in + 0.28 \cdot 11.93\ \text{in}^2 \frac{270\ ksi}{40.32\ in}} = 33.14\ in$$

$$f_{ps} = 270\ ksi\left(1 - 0.28\frac{33.14\ in}{40.32\ in}\right) = 208\ ksi$$

Development of Prestressing Strand (Section 5.11.4 (AASHTO, 2012))

Bonded Strand Section 5.11.4.2 (AASHTO, 2012)

$$l_d \geq k\left(f_{ps} - \frac{2}{3} f_{pe}\right) d_b$$ Equation 5.11.4.2-1 (AASHTO, 2012)

Where:

k is 1.6 for pretensioned members with a depth greater than 24 in

$$l_d \geq 1.6\left(208\ ksi - \frac{2}{3}177.16\ ksi\right)0.5\ in = 71.91\ in$$

The transfer length, l_t, may be taken as 60 strands diameter, so for this case:

$$l_t = 60 \cdot d_b = 60 \cdot 0.5\ in = 30\ in$$

Therefore, for this case:

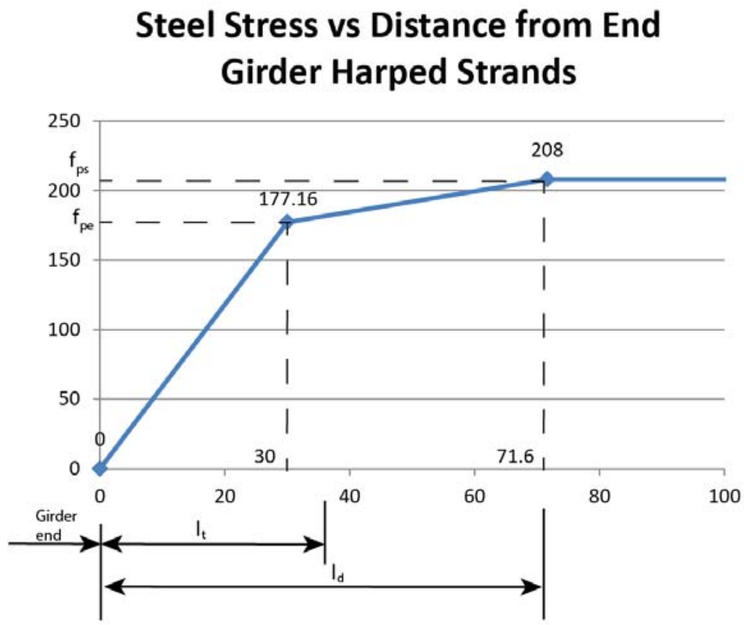

Girder with debonded strands

From the shop drawings in Appendix B, the information that it can be obtained is the following:

- Ø strands = 0.5", Nominal area = 0.153 in^2 (Naaman, 2012)
- Total number of strands = 46, $A_{ps} = 46 \cdot 0.216\ \text{in}^2 = 9.94\ \text{in}^2$
- Tensile strength of prestressing steel (f_{pu}) = 270 ksi
- Type of tendon = low relaxation strand
- Compressive strength of concrete (f'_c) = 7275 psi

- Compressive strength of concrete at release (f'_{ci}) = 6345 psi
- Eccentricity at center line, e_{CL} = 15.01 in
- Eccentricity at end, e_{end} = 13.79 in
- Beam length, l = 110 ft

With the information of the location of the strands, it can be obtained the distance from extreme compression fiber to the centroid of the prestressing tendons (d_p)

$d_p \cdot 46 = 4 \cdot 3.5\ in + 14 \cdot 47.5\ in + 2 \cdot 49.5\ in + 2 \cdot 51.5\ in$

$$d_p = 19.15\ in$$

Prestress losses (Section 5.9.5.1 (AASHTO, 2012))

As discussed in 4.1, the total losses for a pretensioned member is:

$\Delta f_{pT} = \Delta f_{pES} + \Delta f_{pLT}$ Equation 5.9.5.1-1 (AASHTO, 2012)

Elastic Shortening

$\Delta f_{pES} = \frac{E_P}{E_{ct}} f_{cgp}$ Equation 5.9.5.2.3a-1 (AASHTO, 2012)

According to Comment C5.9.5.2.3a (AASHTO, 2012), the loss due to elastic shortening in pretensioned member may be determined by the following alternative equation:

$$\Delta f_{pES} = \frac{A_{ps} \cdot f_{pbt} \cdot \left(I_g + {e_m}^2 \cdot A_g\right) - e_m \cdot M_g \cdot A_g}{A_{ps} \cdot \left(I_g + {e_m}^2 \cdot A_g\right) + \frac{A_g \cdot I_g \cdot E_{ci}}{E_p}}$$

Where:

A_g is the gross area of section, $A_g = 817\ in^2$

E_{ci} is the modulus of elasticity of concrete at transfer, that it can be obtained with equation 5.4.2.4-1 (AASHTO, 2012):

$E_{ci} = 33{,}000 \cdot K_1 \cdot {w_c}^{1.5} \sqrt{f'_{ci}}$

Where:

K_1 is the correction factor for source of aggregate to be taken as 1.0 unless determined by physical test, and as approved by the authority of jurisdiction (AASHTO, 2012), $K_1 = 1$.

w_c is the unit weight of concrete and according to table 3.5.1-1 (AASHTO, 2012), the unit weight for normal weight concrete with $5 \leq f'_c \leq 15$ ksi is $0.140 + 0.001 \cdot f'_c$, since f'_c is 7.3 ksi, $w_c = 0.1473\ kcf$

Therefore,

$E_{ci} = 4699.31\ ksi$

E_p is the modulus of elasticity of prestressing tendons, $E_p = 28{,}500\ ksi$

$e_{m=}e_{CL}$ is the average prestressing steel eccentricity at midspan, $e_m = 15.01\ in$

f_{pbt} is the stress in prestressing steel immediately prior to transfer. According to table 5.9.3-1 (AASHTO, 2012), for low relaxation strands, the stress limit can be taken as $f_{pbt} = 0.75 \cdot f_{pu} = 0.75 \cdot 270\ ksi = 202.5\ ksi$

I_g is the moment of inertia of the gross concrete section that can be obtained from the standard in Appendix A.

$I_g = 299{,}740\ in^4$

$M_g$is the midspan moment due to self-weight of the concrete. The self-weight of the concrete is obtained from the standard Appendix A.

$$M_g = \frac{selfweight \cdot l^2}{8} = \frac{0.851\ klf\ \cdot 110\ ft^2}{8} = 1287.14\ k \cdot ft = 15446\ k \cdot in$$

Therefore,

Δf_{pES}

$$= \frac{9.94\ \text{in}^2 \cdot 202.5\ ksi \cdot (299{,}740\ in^4 + 15.06^2\ in^2 \cdot 817\ in^2) - 15.01\ in \cdot 15446\ k \cdot in \cdot 817\ in^2}{9.94\ \text{in}^2 \cdot (299{,}740\ in^4 + 15.06^2\ in^2 \cdot 817\ in^2) + \frac{817\ in^2 \cdot 299{,}740\ in^4 \cdot 4699.31\ ksi}{28{,}500\ ksi}}$$

$\Delta f_{pES} = 18.57\ ksi$

Creep, Shrinkage and Relaxation of Prestressed Tendons

$\Delta f_{pLT} = 10 \cdot \frac{f_{pi} \cdot A_{ps}}{A_g} \cdot \gamma_s \cdot \gamma_{st} \cdot 12 \cdot \gamma_h \cdot \gamma_{st} + \Delta f_{pR}$ Equation 5.9.5.3-1 (AASHTO, 2012)

The value obtained from equation 5.9.5.3-1 (AASHTO, 2012) is just an approximation. According to Comment C5.9.5.3 (AASHTO, 2012) the values obtained are conservative so article 5.9.5.4 (AASHTO, 2012) can be used instead to obtain these values. However, this article just specifies losses from the time to transfer the girder to when the deck is placed and the time from when the deck is placed until the final time, so for the calculation of prestress losses after release article 5.4.3.2 (AASHTO, 2012) is used.

Creep

Creep coefficient:

$\Psi(t, t_i) = 1.9 \cdot k_s \cdot k_{hc} \cdot k_f \cdot k_{td} \cdot {t_i}^{-0.118}$ Equation 5.4.2.3.2-1 (AASHTO, 2012)

Where:

$k_s = 1.45 - 0.13\left(\frac{V}{S}\right) \geq 1$ Equation 5.4.2.3.2-2 (AASHTO, 2012)

$\frac{V}{S}$ is the volume-to-surface ratio, $\frac{V}{S} = 0.85$

$k_s = 1.34 \geq 1$ OK

$k_{hc} = 1.56 - 0.008H$ Equation 5.4.2.3.2-3 (AASHTO, 2012)

H is the relative humidity (%), $H = 65$

k_{hc}= 1.04

$$k_f = \frac{5}{1 + f'_{ci}}$$ Equation 5.4.2.3.2-4 (AASHTO, 2012)

$k_f = 0.68$

$$k_{td} = \frac{t}{61 - 4f'_{ci} + t}$$ Equation 5.4.2.3.2-5 (AASHTO, 2012)

t is the maturity of concrete (day), it is taken as 1 since that is the time that takes from the moment the concrete is pour to when the strands are released.

$$k_{td} = \frac{1}{61 - 4 \cdot 6345\ psi + 1} = 0.027$$

Therefore,

$$\Psi = 1.9 \cdot 1.34 \cdot 1.04 \cdot 0.68 \cdot 0.027 \cdot 1^{-0.118} = 0.05$$

$$\varepsilon_{ci} = \frac{f_{pbt} \cdot A_{ps}}{A_g \cdot E_{ci}} = \frac{202.5\ ksi \cdot 9.94\ in^2}{817\ in^2 \cdot 4699.31\ \ ksi} = 0.000524$$ (Naaman, 2012)

$$\varepsilon_c = \Psi \cdot \varepsilon_{ci}$$

$\varepsilon_c = 2.62 \cdot 10^{-5}$

$$\Delta f_{ps}(CR) = \varepsilon_c \cdot E_p = 0.75\ ksi$$

Shrinkage

$\varepsilon_{sh} = k_s k_{hc} k_f k_{td} 0.48 \cdot 10^{-3}$ Equation 5.4.2.3.3-1 (AASHTO, 2012)

Where:

$k_{hs} = 2 - 0.014H = 1.09$ Equation 5.4.2.3.3-2 (AASHTO, 2012)

$\varepsilon_{sh} = 1.3 \cdot 10^{-5}$

$\Delta f_{ps}(SH) = \varepsilon_{sh} \cdot E_p = 1.3 \cdot 10^{-5} \cdot 28{,}600\ ksi = 0.37\ ksi$

Relaxation of Prestressing Steel

$$f_{ps}(t) = f_{pbt}\left[1 - \frac{\log_{10}(t)}{K}\left(\frac{f_{pbt}}{f_{py}} - 0.55\right)\right]$$

Where:

$K = 30$ for low relaxation strands

t is duration of loading in hours. $t = 24\ h$ since it is when the strands are released.

f_{py} is the yield strength of prestressing steel (ksi)

From table C5.7.3.1.1-1 (AASHTO, 2012), for a low lax strand:

$$f_{py} = 0.9 \cdot f_{pu} = 0.9 \cdot 270\ ksi = 243\ ksi$$

Therefore,

$$f_{ps}(t) = 202.5\ ksi\left[1 - \frac{\log_{10}(24\ h)}{30}\left(\frac{202.5\ ksi}{243\ ksi} - 0.55\right)\right] = 199.86\ ksi$$

$$\Delta f_{ps}(RL) = f_{pbt} - f_{ps}(t) = 202.5\ ksi - 199.86\ ksi = 2.64\ ksi$$

Total Prestress losses at release

$$f_{pe}(at\ release) = f_{pbt} - \Delta f_{pES} - \Delta f_{ps}(CR) - \Delta f_{ps}(SH) - \Delta f_{ps}(RL)$$

$$f_{pe}(at\ release) = 202.5 - 18.57\ ksi - 0.75\ ksi - 0.37\ ksi - 2.64\ ksi = 180.17\ ksi$$

Stress in Prestressing Steel at Nominal Flexural Resistance (AASTHO 5.7.3.1)

As explained in 4.1.1.4, the average stress in prestressing steel (f_{ps}) may be taken as:

$$f_{ps} = f_{pu}\left(1 - k\frac{c}{d_p}\right)$$

Equation 5.7.3.1.1-2 (AASHTO, 2012)

Where:

$$k = 2\left(1.04 - \frac{f_{py}}{f_{pu}}\right)$$

Equation 5.7.3.1.1-1 (AASHTO, 2012)

To calculate c, the distance from extreme compression fiber to the centroid of the prestressing tendons for components with bonded tendons and unbounded tendons Equation 5.7.3.1.3b (AASHTO, 2012), the simplified analysis:

$$c = \frac{A_{psb} f_{pu+} A_{psu} f_{pe+} A_s f_{s+} A'_s f'_s - 0.85 f'_c (b - b_w) h_f}{0.85 f'_c \beta_1 b_w + k A_{ps} \frac{f_{pu}}{d_p}}$$

Where:

A_{psb} is the area of bonded prestressing steel, $A_{psb} = 36 \cdot 0.216\ in^2 = 7.78\ in^2$

A_{psu} is the area of unbonded prestressing steel, $A_{psu} = 10 \cdot 0.216\ in^2 = 2.16\ in^2$

β_1 is the stress block factor defined in section 5.7.2.2 (AASHTO, 2012). Since f'_c is 7.3 ksi, interpolating $\beta_1 = 0.685$

The value of k can be obtained directly from table C5.7.3.1.1-1 (AASHTO, 2012). For low lax strand, $k = 0.28$

Since the girders tested are Tx54 the following properties from the bridge standards of the Texas Department of Transportation are shown in Appendix A.

$b = 36\ in$, $b_w = 7\ in$, $h_f = 7.5\ in$.

Therefore:

$$c = \frac{7.78\ in^2 \cdot 270\ ksi + 2.16\ in^2 \cdot 180.17 ksi - 0.85 \cdot 7.275\ ksi\ (36\ in - 7\ in) 7.5\ in}{0.85 \cdot 7.275\ ksi \cdot 0.685 \cdot 7 in + 0.28 \cdot 9.93\ in^2 \frac{270\ ksi}{19.15\ in}}$$
$$= 14.3$$

$$f_{ps} = 270\ ksi \left(1 - 0.28 \frac{14.3\ in}{19.15\ in}\right) = 213.5\ ksi$$

Development of Prestressing Strand (Section 5.11.4 (AASHTO, 2012))

Bonded Strand Section 5.11.4.2 (AASHTO, 2012)

Bonded Strand

$l_d \geq k\left(f_{ps} - \frac{2}{3} f_{pe}\right) d_b$ Equation 5.11.4.2-1 (AASHTO, 2012)

Where:

k is 1.6 for pretensioned members with a depth greater than 24 in

$$l_d \geq 1.6\left(213.5\ ksi - \frac{2}{3} 180.17\ ksi\right) 0.6\ in = 89.65\ in$$

The transfer length, l_t, may be taken as 60 strands diameter, so for this case:

$$l_t = 60 \cdot d_b = 60 \cdot 0.6\ in = 36\ in$$

Therefore:

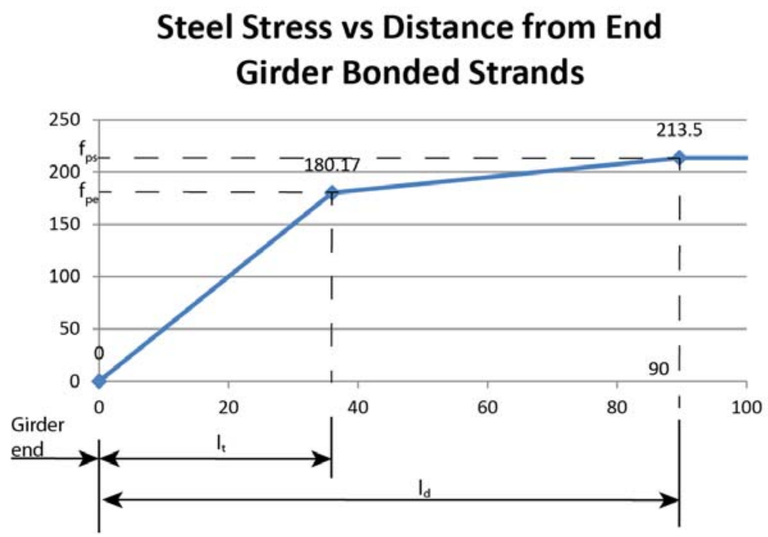

Partially Debonded Strands Section 5.11.4.3 (AASHTO, 2012)

$$l_d \geq 2\left(f_{ps} - \frac{2}{3} f_{pe}\right) d_b = 112\ in$$

$$l_d \geq 2\left(213.5\ ksi - \frac{2}{3}180.17\ ksi\right)0.6\ in$$

Therefore

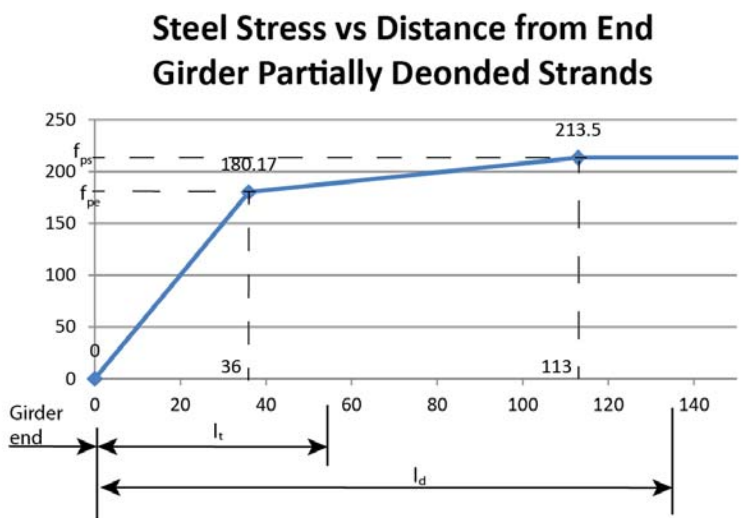

References

AASHTO. (2012). *AASHTO LRFD BRIDGE DESIGN SPECIFICATIONS.* Washington, DC.

ABAQUS, Inc. (2005). ABAQUS Lecture 4 Contact Modeling.

Abdalla, H., & Kennedy, J. B. (1995). Design of prestressed concrete beams with openings. *J. of Sructural Engin.*, 890-898.

Abdalla, O. A., Ramirez, J. A., & Lee, R. H. (1993). *Debonding in pretensioned beams-precast strands, Part 2: simply supported tests.* West Lafayette: FHWA/IN/JHRP-92/25. Joint Highway research Project, Indiana Department of Transportation and Purdue University.

Alenius, M. (2003). *Finite element modelling of composite bridge stability.* Stockholm: Royal Institue of Technology.

Baran, E., French , C., & Shield, C. (2003). *Effects of vertical pre-release cracks on prestressed bridge girders.* Minneapolis: Minnesota Department of Transportation.

Barnes, R. W., Burns, N. H., & Kreger, M. E. (1999). *Development length of 0.6-inch prestresing strand in standard I-shaped pretensioned concrete beams.* Austin: Texas Department of Transportation and the U.S. Department of Transportation, Federal Highway Administration.

Barr, P. J., Halling, M. W., Huffaker, C., & Boyle, H. (2013). *Behavior and analysis of an integral abutment bridge.* Utah Department of Transportation Research Division.

Bechtold, M. (2009). Modeling of steel ropes. *2009 SIMULIA Customer Conference*, (pp. 1-13).

Bullock, W. O., Barnes, R. W., & Schindler, A. K. (2011). *Repair of cracked prestressed concrete girders, I-565, Huntsville, Alabama.* Montgomery: Alabama Department of Transportation and the Highway Research Center.

Chen, L., & Graybeal, B. A. (2010). *Finite element analysis of ultra-high performance concrete: modeling structural performance of an AASHTO Type II girder and a*

2nd generation Pi-girder. McLean: Office of Infrastructure Research & Development.

Chen, L., & Graybeal, B. A. (2012). Modeling structural performance of ultrahigh performance concrete I-girders. *Journal of Bridge Engineering*, 754-764.

Collins, M. P., Mitchell, D., & Macgregory, J. G. (1993). Structural design considerations for high-strength concrete. *Concrete Internation; Design & Construction*, 27-34.

Coogan, D. B. (2006). *Pre-stressing sheath*. Retrieved from http://www.google.st/patents/US7055288

Cook, R. A., Reponen, M. J., & Ansley, M. H. (2008). *Prevention of splitting failure at ends of prestressed beams during fabrication.* Gainesville: University of Florida.

Dassault Systemes Simulia Corp. (2010). *Abaqus 6.10 Abaqus/CAE user's manual.* Providence: Dassault Systemes.

Dassault Systemes Simulia Crop. (2010). *Abaqus 6.10 Example problems manual Vollume II: other applications and analyses.* Providence: Dassault Systemes.

Davis, R. T., Crispino, E. D., Buckner, C. D., & Ozyldirim, C. (n.d.). Serviceability-based design for vertical beam end reinforcement. Virginia Transportation Research Council.

De, S. (n.d.). *Abaqus handout.* Rensselaer Polytechnic Institue.

Deaton, J. B. (2011, Febuary 25th). *Introduction to Abaqus FEA (Tutorial).* Retrieved from http://onlyamodel.com/2011/introduction-to-abaqus-fea-tutorial/

Erdonmez, C., & Imrak, C. E. (2009). Modeling and numerical analysis of the wire strand. *Journal of Naval Science and Engineering*, 30-38.

Erdonmez, C., & Imrak, C. E. (2011). Modeling techniques of nested helical structure based geometry for numierical analysis. *Journal of Mechanical Engineering*, 283-292.

Garimella, R. (n.d.). A practical guide to developing and using mesh and geomery frameworks for advanced meshing and computational software. Los Almos, NM.

Grace, N., Enomoto, T., Baah, P., & Bebawy, M. (2012). Flexural behavior of CFRP precast prestressed decked bulb T-beams. *Journal of Composites for Construction*, 225-234.

Gudlur, P. (n.d.). Introduction to Abaqus CAE. Texas A&M University.

Hein, M. (n.d.). Precast bridge design options that can save money and/or time fromt he fabricators perspective.

Hueste, M., Adil, M., Adnan, M., & Keating, P. (2006). *Impact of LRFD specifications on design of Texas bridges volume 2: prestressed concrete bridge girder design examples.* Austin: Texas Department of Transportation.

Huo, X. S., Crouch, L. K., Ung, F., Zhu, P., & Goodwin, W. A. (2003). *Experimental study of optimal erection schedule of prestressed concrete bridge girders.* Cookeville: Tennessee Department of Transportation and the U.S. Department of Transportation Federal Highway Administration.

Hyzak, M. (2011, February 7-8). TxDOT projects: prefabricated bridge elements and systems. Austin, Texas.

Johanusson, B., Reitzel, P., & Frier, C. (2011). *Numerical Analysis of a reinforced concrete beam in Abaqus 6.10.* Sohugardsholmsvej: Aalborg University.

Kahl, S., & Burgueno, R. (2011). *Effects of debonded strands on the production and performance of prestressed concrete beams.* East Lansing: Federal Highway Administration and the Michigan Department of Transportatoin.

Kennedy, R. H., & Terziyski, J. M. (2004). Experiences with embedded elements in tire modeling. *2004 ABAQUS Users' Conference*, (pp. 373-385).

Khoshnoud, H. R., & Marsono, A. K. (2012). *ABAQUS for reinforced concrete structures workshop linear analysis.* Universiti Teknologi Malasia.

Kim, J.-K., Shin, H.-O., Shin, H.-Y., & Yoon, Y.-S. (2011). Full-scale testing of pretensioned high-strength concrete girders with debonded strands. *Journal of Bridge Engineering*, 847-853.

King, S., & Richards, T. (2013). Solving contact problems with Abaqus. Dassault Systemes.

Kwak, H. G., & Filippou, F. C. (1990). *Finite element analysis of reinforced concrete structures under monotonic loads.* Berkeley: California Department of Transporation and the University of California, Berkeley.

Laskar, A., Howser, R., Mo, Y. L., & Hsu, T. C. (2010). Modeling of prestressed concrete bridge girders. *Earth and Space 2010: Engienering, Science, Construction, and Operation in Challenging Environments* (pp. 2870-2887). American Society of Civil Engineering.

Lee, J., & Fenves, G. L. (1998). Plastic-damage model for cyclic loading of concrete structures. *Jounral of Engineering Mechanics*, 892-900.

Levin, K., & Nilsson, T. (2013). *Evaluation of analysis methods for conventional and steel fibre reinforced concrete slabs.* Goteborg: Chalmers University of Technology.

Lu, X. Z., Teng, J. G., Ye, L. P., & Jiang, J. J. (2007). Intermediate crack debonding in FRP-strngthened RC beams: FE analysis and strength model. *Journal of Composites for Construction*, 161-174.

Lubliner, J., Oliver, J., Oller, S., & Onate, E. (1989). A platic-damage model for concrete. *Int. J. Solids Structures*, 299-326.

Manjunath, M. (2009). *Finite-Element Project ABAQUS Tutorial.*

Miller, D., & Hulsbos, C. L. (1964). *An investication of crack occurrence in the end regions of pretensioned prestressed concrete beams.* Pennsylvania: Fritz Engineering Laboratory.

Moon, D. Y., Zi, G., Kim, J.-h., Lee, S.-J., & Kim, G. (2010). On strain change of prestressing strand during detensioning procedures. *Engineering Structures*, 2570-2578.

Morcous, G., Asaad, S., & Hatami, A. (2013). *Implementation of 0.7 in. diameter strands in prestressed concrete girders.* Omaha: University of Nebraska-Lincoln and the Nebraska Department of Roads.

Naaman, A. E. (2012). *Prestressed Concrete Analysis and Design.* Ann Arbor, Michigan: Techno Press 3000.

Obaidat, Y. T. (2010). *Structural retrofitting of reinforced concrete beams using carbon fibre reinforced polymer.* Lund: Lund University.

Oliva, M. G., & Okumus, P. (2011). *Finite element analysis of deep wide-flanged pre-stressed girders to understand and control end cracking.* Madison: Wisconsin Highway Research Program and the University of Wisconsin-Madison.

Omidi, O., & Lotfi, V. (2010). Finite element analysis of concrete structures using plastic-damage model in 3-D implementation. *International Journal of Civil Engineering* , 187-203.

R, B., & Sun, Y. (2011). *Effects of debonded strands on the production and performance of prestressed concrete beams.* Research report for MDOT.

Reponen, M. (2006). *Prevention of vertical end cracking on prestressed beams during fabrication.* University of Florida.

Roberts , P. (n.d.). *ABAQUS Lecture Part II.*

Roberts, P. (n.d.). *ABAQUS Lecture Part III.*

Russel, B. W., & Burns, N. H. (1993). *Design guidelines for transfer, development and debonding of large diameter seven wire strands in pretensioned concrete girders.* Austin: Texas State Department of Highways and Public Transportation and U.S. Department of Transportation Federal Highway Administration.

Russell, B. W., Burns, N. H., & ZumBrunnen, L. G. (n.d.). Predicting the bond behavior of prestressed concrete beams containing debonded strands. *PCI Journal*, 60-68.

Saibabu, S., Lakshmanan, N., Murthy, A. R., Ganapathi, S. C., Jayaraman, R., & Senthil, R. (2009). External prestressing technique for strengthening of prestressed concrete structural commponents. *Practice Periodical on Structural Design and Construction*, 90-98.

Saiedi, R. (2007). *Load-deflection response of a prestressed concrete T-beam.* Queen's Univsity, Canada.

Shepherd, J. F. (2006). *Hexahedral mesh generation constraints.* Salt Lake City: Scientific Computing and Imaging Institute.

Staples, D. (2006). *South America*. Retrieved from http://www.dstaplesphotography.com/SOUTHAMERICA/Reed%20Boats,%20Lake%20Titicaca,%20Peru.html

Thiagarajan, G., & Roy, S. (2005). *Finite element modeling of reinforced concrete bridge decks with ABAQUS.* Washington: Center for Infrastructure Engineering Studies/UTC program and the U.S. Department of Transportation.

Transportation, T. D. (2014). *Bridge Standards*. Retrieved from http://www.txdot.gov/insdtdot/orgchart/cmd/cserve/standard/bridge-e.htm

Wan, W. (2011). *Assesment of partial strand debonding practice for AASHTO type girders.* Pittsburgh: Swanson School of Engineering.

Wassef, W. G., Smith, C., Clancy, C. M., & Smith, M. J. (2003). *Compreshensive design example for prestressed concrete (PSC) girder superstructure bridge with commentary (in US customary units).* Arlington: Federal Highway Administration.

Wekezer, J., Li, H., Kwasniewski, L., & Malachowski, J. (2004). *Analytical and experimental evaluation of existing Florida DOT bridges.* Florida Department of Transportation.

Biographical Information

Carmen Díaz-Caneja Nieto received her Civil Engineering degree from "Universidad de Burgos" from Spain in the spring of 2011. She started working for the LBJ project in Dallas as an intern in the summer of 2011. She got hired as an engineer and she was admitted to the graduate program in Structural and Applied Mechanics at the University of Texas at Arlington in fall of 2012. At which she completed her Masters of Science in Civil Engineering in the spring of 2014.